THE ORIENTATIONAL FREEDOM OF MOLECULAR PROBES

THE ORIENTATION FACTOR IN INTRAMOLECULAR ENERGY TRANSFER

R. E. DALE, *Paterson Laboratories, Christie Hospital and Holt Radium Institute, Manchester, M20 9BX, Great Britain*
J. EISINGER AND W. E. BLUMBERG, *Bell Laboratories, Murray Hill, New Jersey 07974 U.S.A.*

ABSTRACT The measurement of the efficiency of Förster long-range resonance energy transfer between donor (D) and acceptor (A) luminophores attached to the same macromolecular substrate can be used to estimate the D-A separation, R. If the D and A transition dipoles sample all orientations with respect to the substrate (the isotropic condition) in a time short compared with the transfer time (the dynamic averaging condition), the average orientation factor $<\kappa^2>$ is 2/3. If the isotropic condition is not satisfied but the dynamic averaging condition is, upper and lower bounds for $<\kappa^2>$, and thus R, may be obtained from observed D and A depolarizations, and these limits may be further narrowed if the transfer depolarization is also known. This paper offers experimental protocols for obtaining this reorientational information and presents contour plots of $<\kappa^2>_{min}$ and $<\kappa^2>_{max}$ as functions of generally observable depolarizations. This permits an uncertainty to be assigned to the determined value of R. The details of the D and A reorientational process need not be known, but the orientational distributions are assumed to have at least approximate axial symmetry with respect to a stationary substrate. Average depolarization factors are derived for various orientational distribution functions that demonstrate the effects of various mechanisms for reorientation of the luminophores. It is shown that in general the static averaging regime does not lend itself to determinations of R.

INTRODUCTION

Orientational molecular probes are old tools of the physical chemist. They permitted Perrin to estimate the lifetimes of excited molecules in solution by the use of steady-state polarization spectroscopy some 50 years ago (Perrin, 1926), and more recently have become useful to the biochemist for probing the dynamics and supramolecular structure of anisotropic systems such as membranes (Badley et al., 1973; Kawato et al., 1977). While these and similar uses of orientational probes are based on the interaction between a single transition dipole and the electric vector of a photon, it is the interaction between the two transition dipoles that plays the important role in determining the energy transfer rate between pairs of luminophores.

In most biochemical applications an orientational probe does not have a unique direction in the framework of a quasi-stationary substrate, but has limited freedom of motion with respect to it. This motion may be rapid or slow compared with the emission lifetime, and the range of allowed orientations may be narrowly defined or close to isotropic.

The work presented here develops a model that makes it possible to estimate the effect of orientational freedom of optical probes on experimental parameters such as fluorescence

depolarization and Förster energy transfer rates. The last-named application is of primary concern and makes possible more accurate determinations of intramolecular distances, but a discussion of fluorescence depolarization in terms of models for limited orientational freedom based on several axially symmetrical distribution functions is included. The latter is primarily of heuristic value, because experimental methods for determining such distributions are not available at present, except possibly in oriented systems.

In the 30 years or so since Förster developed an exact quantum mechanical theory of resonance energy transfer for the "very weak" dipole-dipole coupling limit (Förster, 1948, 1951, 1965), an extensive and still rapidly growing literature has described the utilization of the phenomenon to determine intramolecular separations (e.g., recently Wu et al., 1976; Langlois et al., 1976; Shepherd et al., 1976; Wright and Takahashi, 1977; Papadakis and Hammes, 1977; Zukin et al., 1977) and conformational dynamics (Haas et al., 1975, 1977; Ohmine et al., 1977) of mainly biological macromolecules. Further impetus to such studies was undoubtedly provided by the finding that the predicted inverse sixth-power distance dependence of the transfer rate holds closely for several series of oligomers having donor (D) and acceptor (A) moieties bound covalently at their ends, the separation of which depends on the number of intermediate monomer units (Stryer and Haugland, 1967; Conrad and Brand, 1968; Gabor, 1968).

However, as recently emphasized (Eisinger and Dale, 1974; Dale and Eisinger, 1974, 1975), the use of the energy transfer technique as a "spectroscopic ruler" (Stryer and Haugland, 1967) has, with but few possible exceptions (Luk, 1971; Baugher et al., 1974; Maróti and Szalay, 1976), suffered from a lack of knowledge of the relative orientations of the donor and acceptor transition moments, **D** and **A**, upon which the rate of transfer is also strongly dependent—to the extent that, in the most unfavorable case, no energy transfer occurs no matter what the separation[1] (Chang and Filipescu, 1972). Usually, a value for the dipole orientation factor κ^2, corresponding to a dynamic average or sometimes also a completely inappropriate static average (see below and Appendix A) over all orientations of both **D** and **A** is taken to be a good approximation, the tacit or stated assumption being that, even if orientational averaging is limited, extreme values, in particular those near zero, are unlikely. As pointed out earlier (Eisinger and Dale, 1974) and as demonstrated analytically in Appendix B, this argument has no statistical validity; indeed the opposite is true.

The fact that, in many cases, partial averaging of orientations undoubtedly occurs on a time-scale shorter than the transfer time (dynamic averaging), as indicated by some degree of depolarization of D and/or A emission, does not usually justify the use of the isotropic dynamic average value of 2/3, as can readily be seen from examples given previously (Dale and Eisinger, 1975). Fortunately, the assumption of isotropic dynamic orientational averaging for **D** and **A** need not be relied upon, since polarization spectroscopy can be used to obtain information on both the orientational freedom of the donor and acceptor luminophores and on their relative orientations. While this kind of information does not normally yield a unique dynamic average value for the orientation factor, it always delineates realistic upper and lower bound. As will be seen, the range of possible values can, under favorable conditions, be quite

[1]At very close separations, transfer mechanisms other than the very weak coupling dipole-dipole (Förster) transfer considered here predominate (see, e.g., Eisinger et al., 1969). The remarks above and throughout the rest of this text apply only to Förster transfer.

narrow. However, even if it is not, as is the case for a fixed **D-A** configuration, this methodology provides a meaningful estimate of the intrinsic uncertainty in the average value of κ^2 and hence in the D-A separation, without restrictive assumptions about the orientations of **D** and **A**.

ENERGY TRANSFER THEORY

The rate of (one-way) energy transfer in the very weak dipole-dipole coupling limit between D and A moieties of suitable spectroscopic properties is given (Förster, 1948, 1951, 1965) by

$$k_T = (1/\tau_D)(R_0/R)^6, \tag{1}$$

where τ_D is the (singly exponential) decay time of D emission in the absence of A, R is the D-A separation and R_0 is the characteristic (Förster) separation.

$$R_0^6 = C\kappa^2, \tag{2}$$

where C is a constant for the system under investigation, made up of universal constants, a spectral overlap integral, the quantum yield of D in absence of A, and the refractive index of the intervening medium.

The orientation factor κ^2 gives the dependence of the interaction between two electric dipoles on their orientations. It can be defined by

$$\kappa^2 = (\cos\theta_T - 3\cos\theta_D \cos\theta_A)^2, \tag{3}$$

where θ_T is the angle between the **D** and **A** moments, given by

$$\cos\theta_T = \sin\theta_D \sin\theta_A \cos\phi + \cos\theta_D \cos\theta_A \tag{4}$$

in which θ_D, θ_A are the angles between the separation vector **R**, and **D** and **A**, respectively, and ϕ is the azimuth between the planes (**D**, **R**) and (**A**, **R**) (Fig. 1).

For a particular **D-A** pair, i, characterized by an orientation factor κ_i^2, the energy transfer efficiency T_i is given by

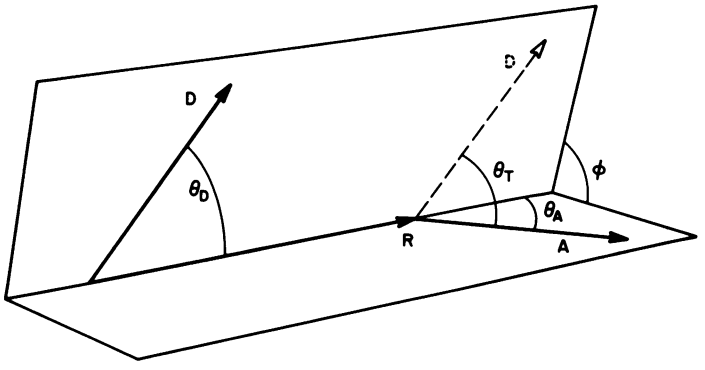

FIGURE 1 Visualization of the angles used to define the relative orientations of the donor and acceptor transition moments (**D** and **A**) and the separation vector (**R**).

$$T_i = k_{Ti}/(\tau_{Di}^{-1} + k_{Ti}) = \kappa_i^2/(C^{-1}R^6 + \kappa_i^2). \quad (5)$$

As has been emphasized elsewhere (Dale and Eisinger, 1976; Eisinger, 1976), only when each D-A pair in the experimental ensemble has the same fixed orientation, or, equivalently, the same extent of dynamic averaging (fast compared with the fluoresence and transfer rates), is it valid to substitute a single or average value for κ_i^2 in Eq. 5, although for low transfer efficiencies this will be a good approximation in the static averaging regime too. This is true independently of whether the transfer efficiency is obtained by steady-state measurements of relative intensities, as has usually been the case, by time-resolved measurements of the decrease in donor lifetime (Wu and Stryer, 1972), or by analysis of the rise and decay of acceptor emission excited by light absorbed by the donor (Schiller, 1975), a method apparently not exploited experimentally to date. Definition of an appropriate unique or dynamic average value of the orientation factor in any given system is usually impossible without independent crystallographic information, which, with few exceptions (Luk, 1971; Baugher et al., 1974; Maróti and Szalay, 1976), is not currently available and even then is of uncertain validity for the solution conditions generally employed in the energy transfer experiment.

An inappropriate isotropic static average value of 0.476 (Galanin, 1955; Maksimov and Rozman, 1962; Steinberg, 1968) has also been quoted quite extensively. Its inapplicability to the problem of intramolecular energy transfer is indicated in Eq. 5, which demonstrates that no average value independent of the D-A separation can be defined, as has been discussed in some detail elsewhere (Dale and Eisinger, 1976). It seems unlikely that isotropic averaging in the static limit will provide an appropriate model in any experimental single D-A pair system, but the effect of this is examined in Appendix A, included less for its practical applicability than to illustrate how much energy transfer efficiencies can be affected by the orientational averaging regime.

Fluoresence Depolarization

It has been known for more than 50 years that in general luminescence is partially polarized. This is true even for an assembly of randomly oriented luminophores in solution excited by polarized or, indeed, unpolarized light, provided only that complete thermal orientational relaxation does not occur in the interval between excitation and emission. The explanation of this phenomenon of photoselection (Albrecht, 1961) is that molecules whose transition moments are aligned closer to the direction of the electric vector of the exciting light (and therefore more nearly perpendicular to its propagation direction) are preferentially selected for excitation even when the exciting light is unpolarized. In many cases, certainly in most cases of interest in energy transfer studies, the observed polarization properties of the system can be well described in terms of specific transition moments associated with absorption and emission. The extent of depolarization of the emission transition moment from such a photoselected assembly reflects the change in orientation between the initial absorption and final emission transitions.

The most useful measure of the extent of polarization is the emission anisotropy (EA) r introduced relatively recently (Jabłoński, 1960), but used implicity much earlier (Perrin, 1936). This quantity may be defined by

$$r = (I_V - I_H)/I, \tag{6}$$

where I_V, I_H are the vertically and horizontally polarized components of the emission observed at right angles to an arbitrarily polarized excitation beam, the excitation and emission directions being in the horizontal plane. I represents the sum of any three orthogonally polarized intensities and corresponds to the total emission intensity. For V-polarized excitation, which is usually employed since it gives rise to the maximum EA,

$$I = I_V + 2I_H, \tag{7}$$

since the symmetry of the system dictates that the third (unobserved) polarized component of the emission intensity is equal to the (observed) H-polarized component. Under these conditions the EA attains its limiting value of 0.4 if the absorption and emission moments coincide in the luminophore framework, and no extrinsic reorientation due, for instance, to rotation occurs.[2] If a series of depolarizing events intervenes between absorption and emission and each reorientation is azimuthally isotropic with respect to the preceding one, the EA is lowered from this limiting value, and according to Soleillet's theorem (Soleillet, 1929)

$$r = 0.4 \prod_i d_i \tag{8}$$

where d_i represents depolarization factors (Soleillet, 1929; Perrin, 1936) defined by

$$d_i = \tfrac{3}{2} \cos^2 \theta_i - \tfrac{1}{2}, \tag{9}$$

θ_i being the angle by which the transition moment is changed in the i^{th} depolarization step. More commonly, a distribution of θ values is of interest, and the use of an average depolarization factor

$$<d>_i = \tfrac{3}{2} <\cos^2 \theta>_i - \tfrac{1}{2} \tag{10}$$

is appropriate.

Thus, in energy transfer between D and A fixed with respect to an immobile substrate, for instance, the observed EA for the transferred excitation energy (r_T) is

$$r_T = 0.4 \, (\tfrac{3}{2} \cos^2 \theta_T - \tfrac{1}{2}) = 0.4 \, d_T. \tag{11}$$

The azimuthal averaging that justifies the use of Soleillet's theorem is assured in this case, because in a solution containing an ensemble of **D-A** pairs there exists an axially isotropic distribution of planes containing θ_T about **D**.

---

[2]In principle these vectors are coincident in a lowest-lying nondegenerate transition. As discussed elsewhere (Dale and Eisinger, 1975), cases of excitation or transfer into higher transitions, the moments of which are not parallel to that of emission, do not lend themselves to the analysis of the energy transfer problem proposed here. Axially symmetric degeneracy of transitions contribute to the overall depolarization process, according to Eqs. 8 and 9, while slight planar degeneracy, such as may account for limiting EA values less than 0.4 even in dilute rigid or highly viscous solutions, can be treated in the same way, at least to first order. In the following, therefore, both **D** and **A** will be taken to represent coincident, i.e. nondegenerate, absorption and emission transition moment vectors.

For many applications of interest to the biochemist or polymer chemist, a realistic model for an ensemble of identical macromolecules in solution, each endowed with an equivalent D-A pair, is one in which both **D** and **A** have some degree of reorientational freedom with respect to a rigid macromolecular framework that defines their fixed separation. The macromolecule itself may be free to rotate in the supporting solvent, but the effect of slow substrate rotation, considered artifactual in the present analysis, can be accounted for experimentally (Dale and Eisinger, 1975). This and the effect of segmental flexibility, which may alter the D-A separation (Cantor and Pechukas, 1971; Grinvald et al., 1972; Haas et al., 1975, 1977; Ohmine et al., 1977), have been discussed elsewhere (Dale and Eisinger, 1975, 1976) and are excluded from further consideration here.

In the following, this model in the dynamic averaging limit is analyzed to investigate the effects of limited orientational freedom of **D** and **A** on the orientation factor in Förster energy transfer and on the transfer depolarization. It is shown how estimates of upper and lower bounds for the average value of the orientation factor may be obtained by utilizing the information available from polarization measurements.

Transfer Depolarization

Fig. 2 illustrates the model employed for calculating the depolarization resulting from energy transfer between two luminophores with limited orientational freedom. The axially symmetric orientational distributions of the donor and acceptor transition moments are indicated by cones with axes $\mathbf{D}^x$ and $\mathbf{A}^x$, respectively. Fig. 2 *a* shows schematically the three depolarizing events, those due to reorientation of **D** and **A** and that brought about by transfer between them. The overall depolarization between $\mathbf{D}_i$ and $\mathbf{A}_j$ depends only on the relative orientation of these two vectors, specifically on $\cos \theta_{ij} = (\mathbf{D}_i \cdot \mathbf{A}_j)$ and not at all on the intermediate orientations $\mathbf{D}_j$ and $\mathbf{A}_i$. In the dynamic reorientational limit, all possible orientations corresponding to $\mathbf{D}_j$ and $\mathbf{A}_i$ are explored many times during the transfer period so that the transfer rate does not depend on either the initial acceptor orientation $\mathbf{A}_i$ into which the transfer of excitation occurs or the final donor orientation $\mathbf{D}_j$ from which emission occurs. The average transfer depolarization is therefore simply that of all $\mathbf{D}_i$, $\mathbf{A}_j$ pairs, each pair contributing with the same weight to the average, so that

$$\langle d_T \rangle = \tfrac{3}{2} \langle \cos^2 \theta_{ij} \rangle - \tfrac{1}{2}. \tag{12}$$

The azimuthal averaging implied in Eq. 12 is ensured by the fact that in a solution of identical D, A-labeled macromolecules, every vector $\mathbf{D}_i$, fixed at the moment of excitation in the laboratory coordinate system, has a uniform distribution of planes containing θ_{ij} about it.

Under the circumstances detailed above, the transfer depolarization process depicted in Fig. 2 *b*, involving reorientation of $\mathbf{D}_i$ to the axial orientation $\mathbf{D}^x$ followed by transfer to the acceptor in its axial orientation $\mathbf{A}^x$ and reorientation to $\mathbf{A}_j$, is entirely equivalent to that in Fig. 2 *a* and may formally replace it. Since $\mathbf{D}_i$ and $\mathbf{A}_j$ are axially symmetrically distributed about $\mathbf{D}^x$ and $\mathbf{A}^x$, respectively, and the azimuthal orientation of $\mathbf{A}^x$ about $\mathbf{D}^x$ (being a particular case of $\mathbf{A}_j$ about $\mathbf{D}_i$) is random, Soleillet's theorem (Eq. 8) applies, and the average transfer

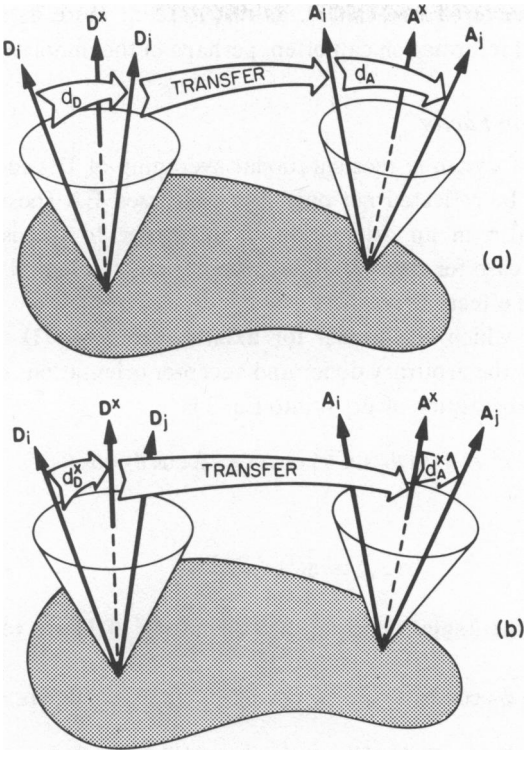

FIGURE 2 (*a*) Schematic representation of the three depolarizing steps after the absorption of excitation energy by the donor: donor depolarization, transfer depolarization, and acceptor depolarization. It is shown in the text that the depolarization corresponding to these steps is the same as in the three depolarizing events shown in *b*: axial depolarization of the donor, depolarization due to transfer between the axes of the orientational distributions of **D** and **A**, and axial depolarization of the acceptor.

depolarization factor is the product of the three depolarization factors, corresponding to the three depolarizing events depicted in Fig. 2 *b*:

$$<d_T> = <d_D^x> d_T^x <d_A^x>, \tag{13}$$

where $<d_D^x>$, $<d_A^x>$ will be referred to as the axial depolarization factors for D and A, respectively, and d_T^x as the axial transfer depolarization factor associated with their axial (mean) orientations, that is,

$$d_T^x = \tfrac{3}{2}\cos^2\Theta_T - \tfrac{1}{2}, \tag{14}$$

where Θ_T is the angle between $\mathbf{D}^x$ and $\mathbf{A}^x$ (cf. Fig. 3). A formal derivation of Eq. 13 is given in the following section.

As will be shown below, the axial depolarization factors may be obtained from observed depolarizations of D and A excited and observed separately. From these and $<d_T>$ it is possible to determine d_T^x, and, by use of Eq. 14, Θ_T, the angle between the axes of the D and A orientational distributions. This determination is not always unique, because in a certain range of values, the signs of $<d_D^x>$ and $<d_A^x>$ obtained in this way are indeterminate. In

such situations Θ_T is rendered two-valued, as discussed in more detail later. Nevertheless, unambiguous structural information can often, perhaps in the majority of cases, be obtained.

The Orientation Factor

Clearly, some degree of dynamic reorientational averaging of **D** and **A** or both about their mean orientations will be reflected not only in a decreased EA (positive or negative) after energy transfer, but also in an orientation factor closer to the isotropic value of 2/3. Furthermore, as is the case for fixed **D** and **A** orientations (Dale and Eisinger, 1974, 1975), the magnitudes of these effects are related.

Consider Fig. 3, in which the model for axially symmetric **D** and **A** distributions is illustrated in detail. For the arbitrary donor and acceptor orientations defined, the orientation factor determined by substitution of Eq. 4 into Eq. 3 is

$$\kappa^2 = (\sin\theta_D \sin\theta_A \cos\phi - 2\cos\theta_D \cos\theta_A)^2, \tag{15}$$

where the azimuth ϕ is

$$\phi = \Phi + \phi_A - \phi_D. \tag{16}$$

It is readily seen that the angles defining the orientation of **D** are related by the following identities:

$$\sin\phi_D \cos\phi_D = \sin\Theta_D \cos\psi_D - \cos\Theta_D \sin\psi_D \cos\gamma_D \tag{17}$$

$$\cos\theta_D = \cos\Theta_D \cos\psi_D + \sin\Theta_D \sin\psi_D \cos\gamma_D \tag{18}$$

along with the equivalent identities for **A**. On substitution of Eqs. 16–18 into Eq. 15, expansion, collection of terms and averaging over the azimuthal angles γ_D and γ_A,

$$<\cos\gamma> = <\sin\gamma> = <\cos\gamma \sin\gamma> = 0, \tag{19}$$

$$<\cos^2\gamma> = <\sin^2\gamma> = 1/2, \tag{20}$$

and over the appropriate ranges of ψ_D and ψ_A, one sees that the (dynamic) average value of the orientation factor is

$$<\kappa^2> = \kappa^{x2} <d_D^x> <d_A^x> + \tfrac{1}{3}(1 - <d_D^x>) + \tfrac{1}{3}(1 - <d_A^x>) + \cos^2\Theta_D <d_D^x> (1 - <d_A^x>) + \cos^2\Theta_A <d_A^x> (1 - <d_D^x>), \tag{21}$$

in which

$$\kappa^{x2} = (\sin\Theta_D \sin\Theta_A \cos\Phi - 2\cos\Theta_D \cos\Theta_A)^2 \tag{22}$$

is the axial orientation factor defined for the axial (mean) orientations $\mathbf{D}^x$ and $\mathbf{A}^x$, while

$$<d_D^x> = \tfrac{3}{2} <\cos^2\psi_D> - \tfrac{1}{2} \tag{23}$$

and

$$<d_A^x> = \tfrac{3}{2} <\cos^2\psi_A> - \tfrac{1}{2}. \tag{24}$$

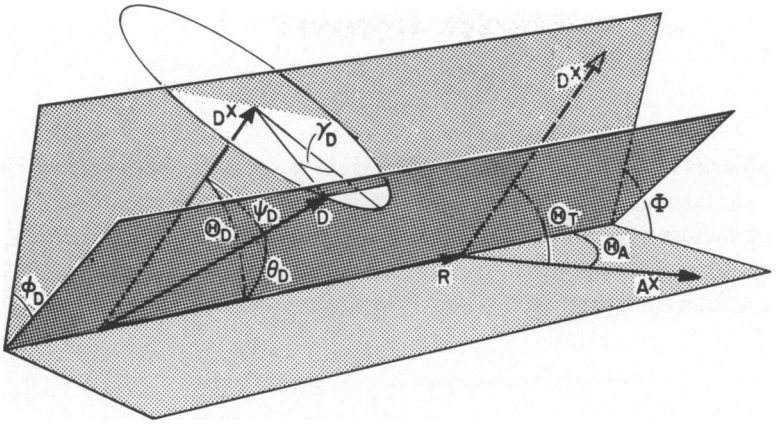

FIGURE 3 Analogous to Fig. 1, except that the place of the **D** and **A** transition moments is taken by the symmetry axes ($\mathbf{D}^x$ and $\mathbf{A}^x$) of their distributions. This model is used in evaluating the orientation and depolarization factors in terms of the angular parameters ψ_D and γ_D, indicated along with the corresponding acceptor parameters ψ_A and γ_A, omitted here for clarity.

By using the same averaging procedures on $\cos^2 \theta_T$ defined in Eq. 4, the overall (dynamic) average transfer depolarization factor is readily shown to be

$$\begin{aligned} \langle d_T \rangle &= \tfrac{3}{2} \langle \cos^2 \theta_T \rangle - \tfrac{1}{2} \\ &= (\tfrac{3}{2} \langle \cos^2 \psi_D \rangle - \tfrac{1}{2})\,(\tfrac{3}{2} \cos^2 \Theta_T - \tfrac{1}{2})\,(\tfrac{3}{2} \langle \cos^2 \psi_A \rangle - \tfrac{1}{2}), \end{aligned} \quad (25)$$

where

$$\cos^2 \Theta_T = (\sin \Theta_D \sin \Theta_A \cos \Phi + \cos \Theta_D \cos \Theta_A)^2. \quad (26)$$

Eq. 25 is seen to be identical with Eq. 13, derived by the direct application of Soleillet's theorem.

Maximum and Minimum Values of the Orientation Factor

It is clear from Eqs. 13 or 25 that, given values of $\langle d_T \rangle$, $\langle d_D^x \rangle$, and $\langle d_A^x \rangle$, all of which may in principle be measured experimentally, Θ_T can be determined. As can be seen by comparing Eqs. 22 and 26, some limitation is thereby imposed on the otherwise indeterminate functions of the angles Θ_D, Θ_A, and Φ appearing in Eq. 21. Differentiation with respect to two of these variables, the third being determined by the fixed value of Θ_T, will establish conditions for maximum and minimum values of $\langle \kappa^2 \rangle$.

Thus, differentiating Eq. 21 twice with respect to the azimuthal angle Φ shows that, if the two axial depolarizations have the same sign, a minimum occurs when κ^{x2} is identically zero. Either Θ_D or Θ_A may then be eliminated, and double differentiation with respect to the other angle reveals that $\langle \kappa^2 \rangle$ has the minimum value

$$\begin{aligned} \langle \kappa^2 \rangle_{\min} = \tfrac{2}{3} \{1 &- (\langle d_D^x \rangle + \langle d_A^x \rangle)/2 \\ &+ \cos \Theta_T [\langle d_D^x \rangle \langle d_A^x \rangle (1 - \langle d_D^x \rangle)(1 - \langle d_A^x \rangle)]^{1/2}\}, \end{aligned} \quad (27)$$

when

$$\cos^2 \Theta_1 = \frac{\cos \Theta_T}{3} \left[\frac{<d_2^x> (1 - <d_1^x>)}{<d_1^x> (1 - <d_2^x>)} \right]^{1/2} \tag{28}$$

where the subscripts (1, 2) refer either to (D, A) or to (A, D). As a result of the condition given in Eq. 28, the sign of the term containing Θ_T in Eq. 27 is always positive. If the axial depolarization factors have opposite signs, a maximum with respect to Φ obtains, but it leads only to a minimum with respect to Θ_D or Θ_A, and then only if this angle, say Θ_1, is zero, implying the unique configuration $\Theta_2 = \Theta_T = \pi/2$.

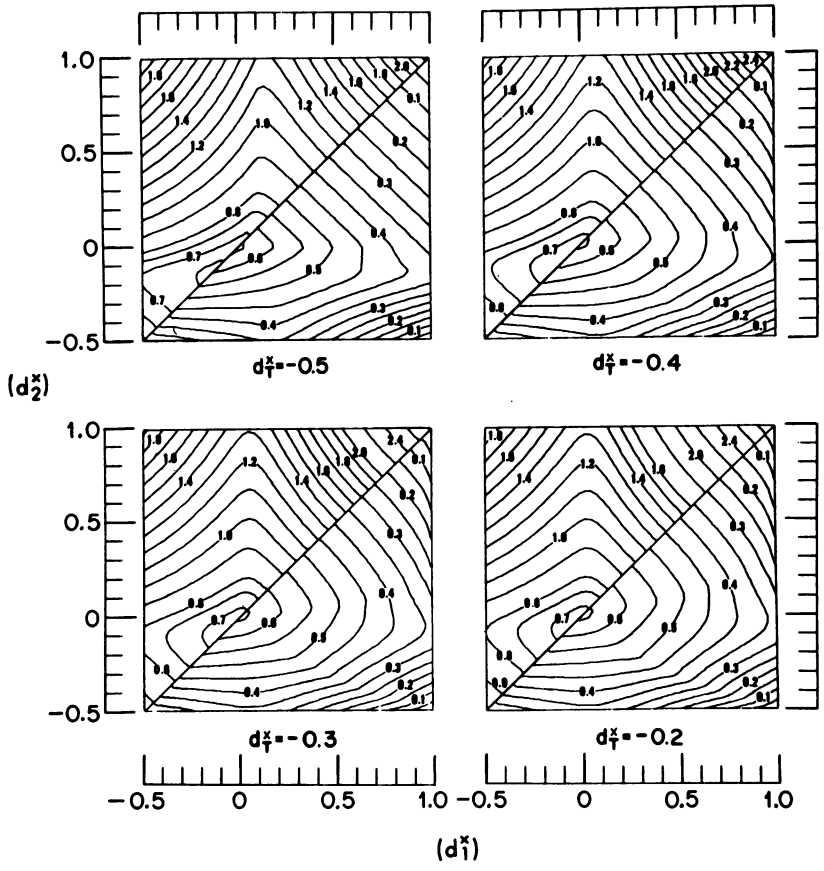

FIGURE 4 Contour plots for obtaining extreme values of $<\kappa^2>$ consistent with the observed donor, acceptor, and transfer depolarization factors. Contours for the minimum and maximum values appear in the lower right and upper left halves of the diagrams, each for a particular value of d_T^x, the axial transfer depolarization factor defined in Eqs. 13 and 14. The contours are plotted as functions of $<d_1^x>$ and $<d_2^x>$, the dynamically averaged axial depolarization factors of the two luminophores between which transfer occurs. These axial depolarization factors are obtained from the observed donor and acceptor depolarization factors by using Eq. 33. If one or both of the observed depolarization factors are less than 1/4, there is a degeneracy in the sign of the axial depolarization factors and the appropriate sign must be chosen to obtain the absolute upper and lower limit of $<\kappa^2>$ from these contour plots, as discussed in the text.

On the other hand, maxima and minima with respect to $\Phi = 0$ or π occur for all relative values of $<d_D^x>$ and $<d_A^x>$. Θ_D and Θ_A are related to Θ_T in both limits of Φ by

$$\cos \Theta_2 = \cos \Theta_T \cos \Theta_1 + \sin \Theta_T \sin \Theta_1, \tag{29}$$

so that

$$\kappa^x = \cos \Theta_T (3 \cos^2 \Theta_1 - 1) + 3 \sin \Theta_T \cos \Theta_1 \sin \Theta_1, \tag{30}$$

in Eq. 21 for $<\kappa^2>$. No attempt was made to determine analytical maxima and minima with respect to Θ_D or, equivalently, Θ_A, for this function. Instead, they were found to a good approximation by searching through the variable from 0 to π, confining Θ_T to the range $(0 \leq \Theta_T \leq \pi/2)$, equivalent to searching the physically relevant range $(0, \pi/2)$ of the variable for both possible transfer angles, Θ_T and $(\pi - \Theta_T)$. Absolute maxima for any given values of the axial depolarization factors were obtained directly in this way, as were minima when $<d_D^x>$

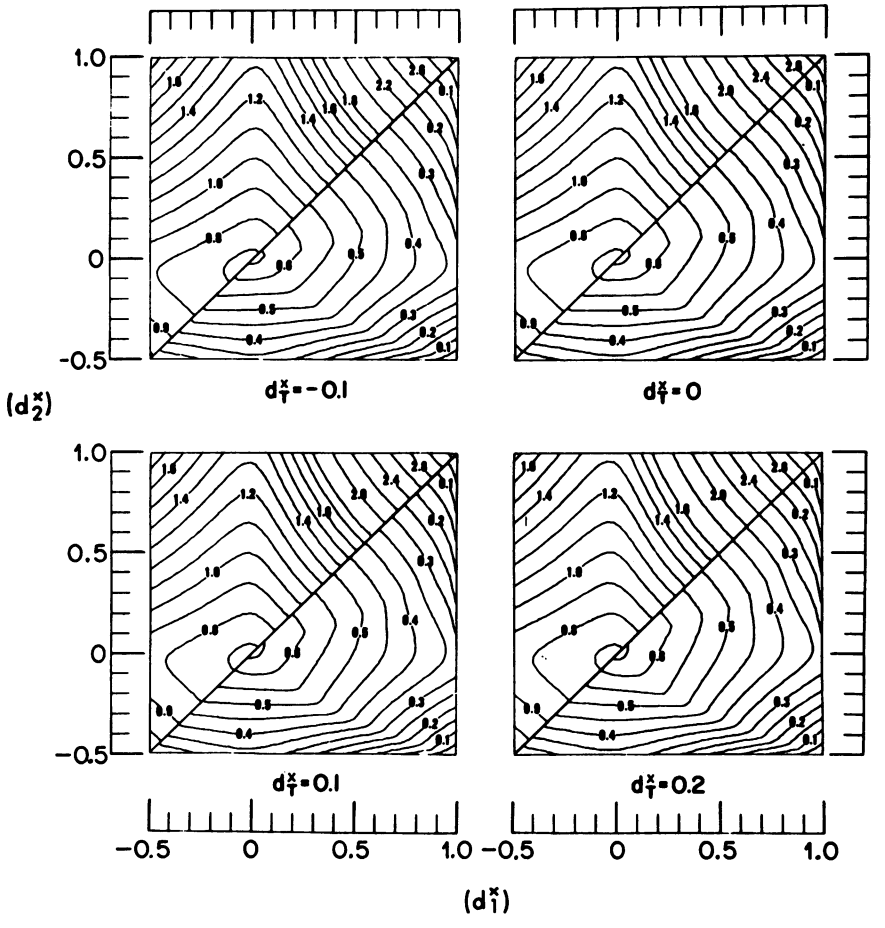

FIGURE 5 Contour plots for obtaining upper and lower limits of $<\kappa^2>$, as in Fig. 4, but for $d_T^x = -0.1$, 0, 0.1, and 0.2.

and $<d_A^x>$ have opposite signs. Absolute minima when these depolarization factors have the same sign required comparison of the values derived from the search with those obtained from Eq. 27.

This searching and checking procedure was accomplished by computer, and the results were fed directly into a plotting program which, for fixed values of d_T^x, generated contours of $<\kappa^2>_{max}$ and $<\kappa^2>_{min}$ as a function of the two axial depolarization factors. Since these contour plots are invariant with respect to inversion of $<d_D^x>$ and $<d_A^x>$, they are symmetrical with respect to reflection on the diagonal, and the contours for $<\kappa^2>_{min}$ and $<\kappa^2>_{max}$ may be combined in a single square diagram. They are displayed in Figs. 4–7 for steps in the axial transfer depolarization factor of 0.1 in the range ($-0.5 \leq d_T^x \leq 1$) as functions of $<d_1^x>$ and $<d_2^x>$, where again the subscripts (1, 2) refer to either (D, A) or (A, D). In Fig. 8 the same contour plots for d_T^x values of -0.5, 0, 0.5, and 1 are given, and the regions in which the isotropic assumption of $<\kappa^2> = \frac{2}{3}$ leads to appreciable errors in the derived intramolecular separation R are also indicated.

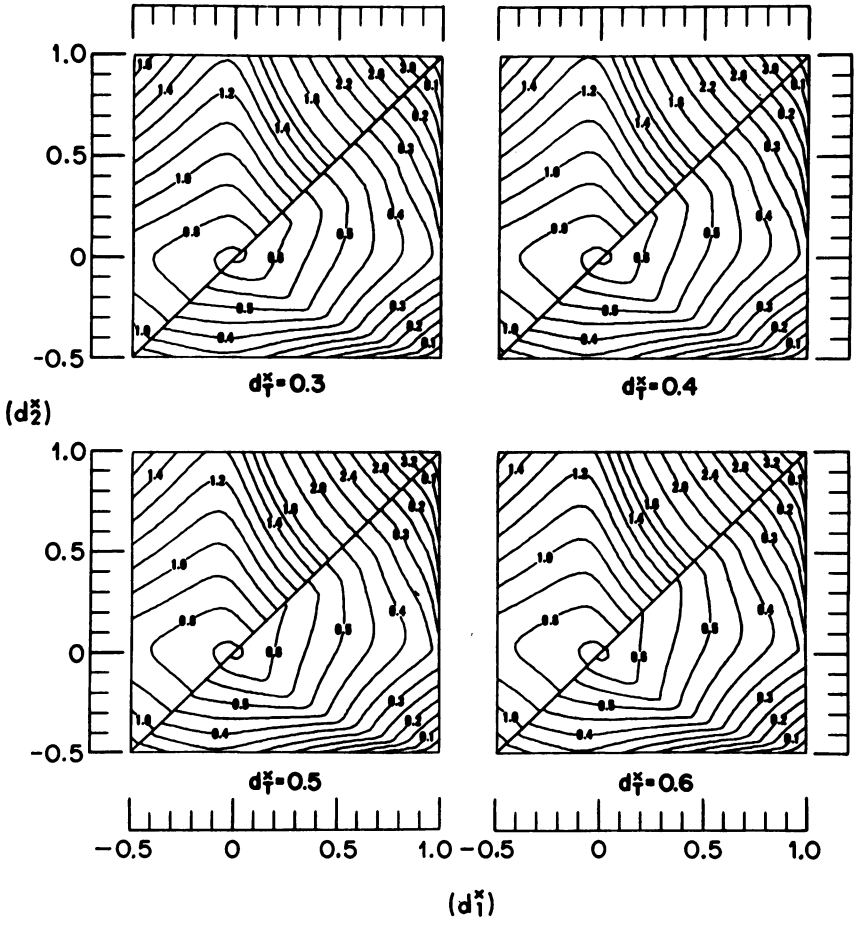

FIGURE 6 Contour plots for obtaining upper and lower limits of $<\kappa^2>$, as in Fig. 4, but for $d_T^x = 0.3$, 0.4, 0.5, and 0.6.

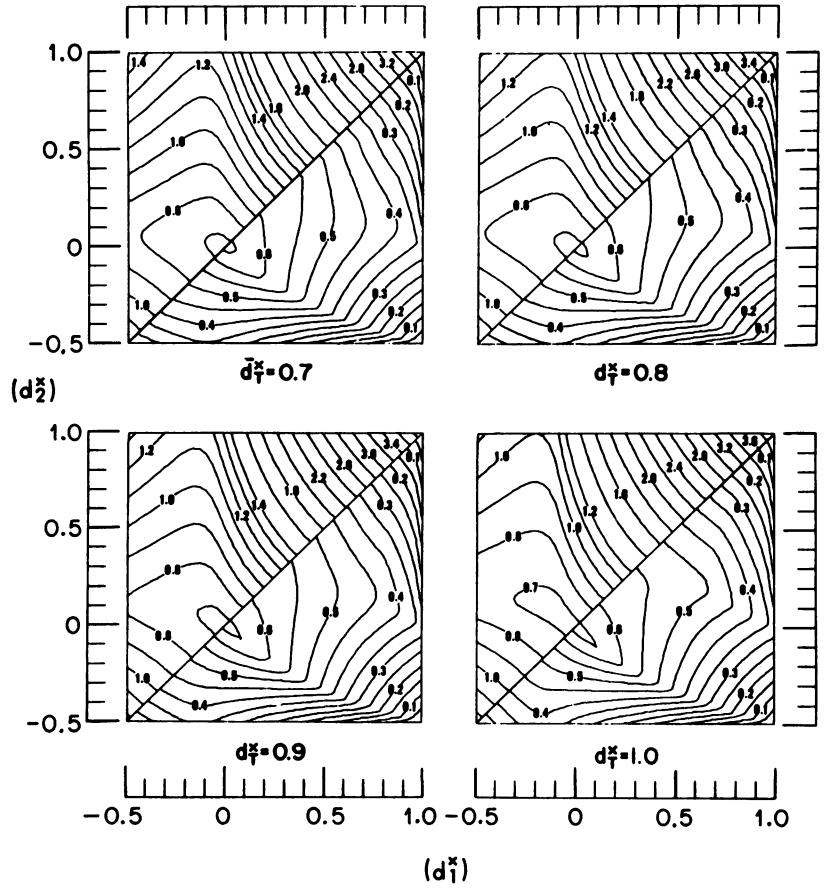

FIGURE 7 Contour plots for obtaining upper and lower limits of $<\kappa^2>$, as in Fig. 4, but for $d_T^x = 0.7$, 0.8, 0.9, and 1.0.

When the transfer depolarization is not determined, it is inconvenient to use these plots. Accordingly, the contour plot of Fig. 9 displays maxima and minima of $<\kappa^2>$ obtained by extending the search procedure used above to cover the range of Θ_T values also. Stippling is again used to indicate the regions in the $<d_1^x>$, $<d_2^x>$ space in which the isotropic assumption leads to inaccurate values of R.

When both axial depolarization factors are positive, particularly simple expressions apply. Inspection of Eqs. 21 and 27 shows that under these conditions the maximum and minimum values of $<\kappa^2>$ are

$$<\kappa^2>_{max} = \tfrac{2}{3}(1 + <d_D^x> + <d_A^x> + 3<d_D^x><d_A^x>) \tag{31}$$

and

$$<\kappa^2>_{min} = \tfrac{2}{3}[1 - (<d_D^x> + <d_A^x>)/2]. \tag{32}$$

These two limiting cases correspond to $\mathbf{D}^x$, $\mathbf{A}^x$, and $\mathbf{R}$ being parallel-in-line and mutually perpendicular, respectively, cases presented previously for a specific model of dynamic distributions of $\mathbf{D}$ and $\mathbf{A}$ (Eisinger and Dale, 1974; Dale and Eisinger, 1974, 1975).

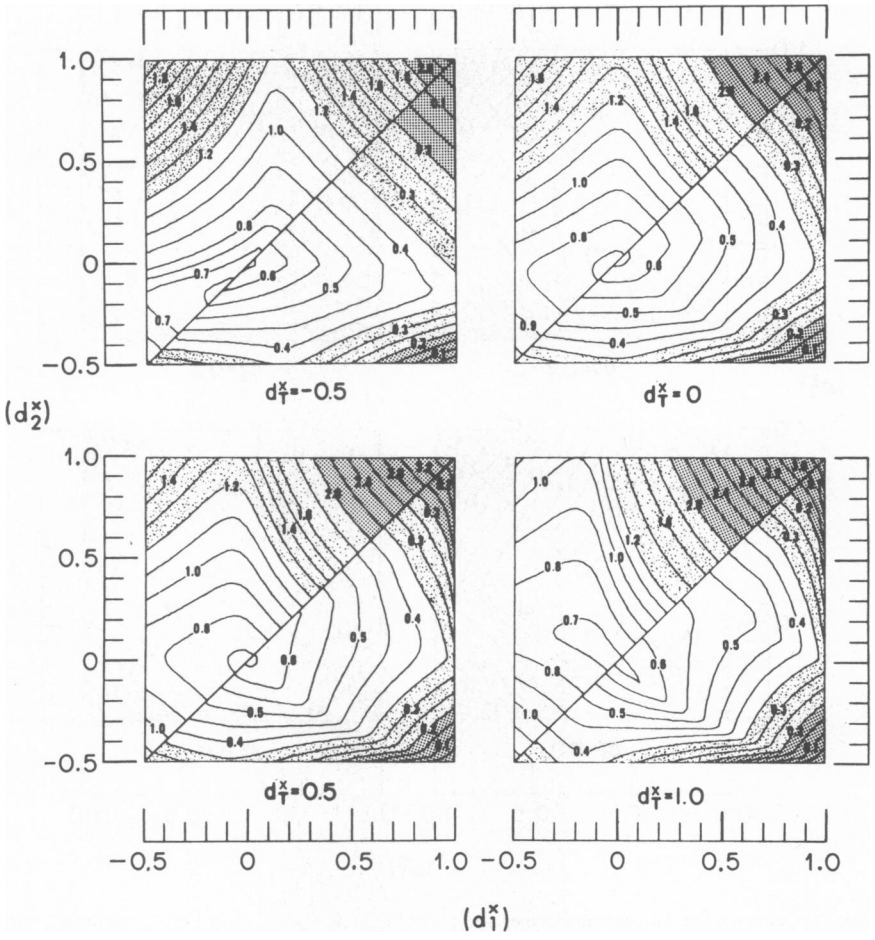

FIGURE 8 Contour plots for obtaining upper and lower limits for $<\kappa^2>$, as in Fig. 4, but for $d_T^x = -0.5$, 0, 0.5, and 1.0. Stippled regions of the contour plots indicate the uncertainty in R, the donor-acceptor separation, which results from using $<\kappa^2> = \frac{2}{3}$, instead of the appropriate $<\kappa^2>_{min}$ and $<\kappa^2>_{max}$ values. The heavily and lightly stippled regions correspond to errors in R of more than 20% and between 10 and 20%, respectively, while the error is less than 10% in the unstippled domain. It is of course negligibly small when the luminophore depolarization factors are near zero, corresponding to orientational isotropy and to $<\kappa^2>_{min} \simeq <\kappa^2>_{max} \simeq \frac{2}{3}$. The errors become considerable for depolarization factors near unity, which correspond to luminophores with little or no orientational freedom with respect to the substrate.

As was mentioned before and will be demonstrated below, axial depolarization factors with values less than 0.5 may be degenerate in sign. However, because it is possible to assign a negative value in some cases, all combinations of signs have been included in all the contour plots. In general, though, each appropriate combination of signs should be checked to ensure that the absolute maximum and minimum of $<\kappa^2>$ consistent with the data are selected. As an example, take $<d_T> = 0.064$, $<d_D^x> = 0.8$, and $<d_A^x> = \pm 0.4$. According to Eqs. 13 and 25 this corresponds to $d_T^x = \pm 0.2$ (Figs. 4 and 5). Minimum and maximum values of 0.35 and 1.85 are obtained when $<d_A^x>$ and d_T^x are both positive, and with both negative the extrema are 0.20 and 1.6. The absolute limiting values for $<\kappa^2>$ are therefore 0.20 and 1.85,

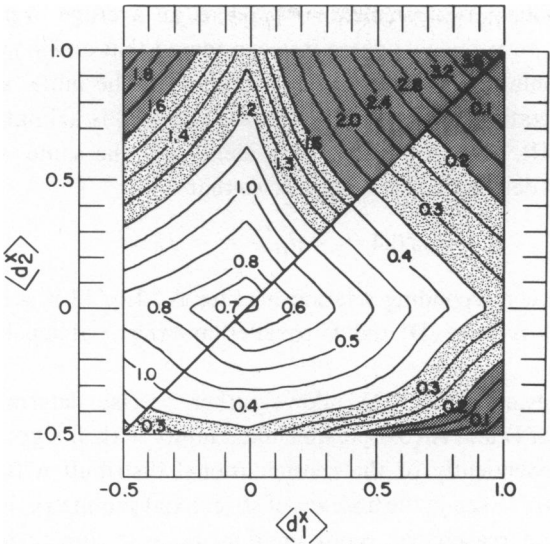

FIGURE 9 Contour plot similar to those shown in Figs. 4–8, but applicable in situations in which $\langle d_T \rangle$, and hence d_T^x, is unknown. It is obtained by maximizing and minimizing Eq. 21 and can be seen to lead to larger ranges between $\langle \kappa^2 \rangle_{min}$ and $\langle \kappa^2 \rangle_{max}$ than the plots of Figs. 4–8. In the heavily stippled regions the error in R resulting from the use of $\langle \kappa^2 \rangle = \frac{2}{3}$ instead of the indicated $\langle \kappa^2 \rangle_{min}$ and $\langle \kappa^2 \rangle_{max}$ is greater than 20%. It is between 10% and 20% in the lightly stippled regions and less than 10% in the unstippled ones.

corresponding to an uncertainty in the derived intramolecular separation of approximately $\pm 18\%$ about the mean value. For this case, if $\langle d_T \rangle$ and therefore d_T^x is unknown, $\langle \kappa^2 \rangle$ lies between 0.20 and 2.1, so that R can be obtained with little loss of accuracy (Fig. 9). By and large, estimation of d_T^x becomes less helpful the greater the extent of depolarization of D and A emission, as is immediately evident on comparing values for $\langle \kappa^2 \rangle_{max}$ and $\langle \kappa^2 \rangle_{min}$ along the diagonals of the contour plots shown in, for example, Fig. 8.

Axial and Observed Depolarization Factors

Because $\langle d_D^x \rangle$ and $\langle d_A^x \rangle$ are used to parametrize the contour plots for $\langle \kappa^2 \rangle_{min}$ and $\langle \kappa^2 \rangle_{max}$, while experiments yield $\langle d_D \rangle$ and $\langle d_A \rangle$, a general relationship between axial and observed depolarization factors is needed and is derived in this section. Due to the dynamic orientational averaging postulated above, the emission of A excited directly will be depolarized, i.e., the apparent r_0 values derived either from a Perrin plot or from nanosecond time-resolved EA decay measurements will be less than the fundamental one of 0.4. Analogously, the same is true for the emission from D alone, either in the absence or the presence of energy transfer.[3] From the donor geometry schematized in Fig. 2, it is evident that

[3]A difference in the apparent r_0 for these two conditions indicates either (*a*) all or part of the reorientation is on the same time scale as transfer (r_0 is always larger, i.e. less depolarization occurs, when transfer competes with deactivation because the emission lifetime shortens) or (*b*) presence of the acceptor has induced some conformational change affecting the range over which dynamic reorientation can occur (r_0 may be larger or smaller in the presence of the acceptor). The second condition obtains also for acceptor emission in the presence or absence of donor.

the directly observed depolarization factor $<d_D>$ is an average over all initial and final orientations $\mathbf{D}_i$ and $\mathbf{D}_j$, respectively, where it is considered that emission rather than transfer takes place at the orientation $\mathbf{D}_j$. Because once again only the initial and final orientations determine the depolarization, and each orientation $\mathbf{D}_i$ and $\mathbf{D}_j$ is azimuthally averaged about the axial orientation $\mathbf{D}^x$, and moreover covers identically the same reorientational range, Soleillet's theorem in a degenerate form applies, so that

$$r_{0D}/0.4 = <d_D> = <d_D^x>^2 \tag{33}$$

obtains along with the corresponding relationships for A.[4] Eq. 33 is seen to be equivalent to Eqs. 13 and 25 when d_T^x is unity ($\mathbf{D}^x$ and $\mathbf{A}^x$ parallel) and the axial depolarization factors of D and A are the same.

The simple relationship of Eq. 33 allows rather precise determination of the axial depolarization factors of D and A (bar possible uncertainty in their signs in the range $-0.5 \leq <d_{D,A}^x> \leq 0.5$) independently of the reorientational distribution function as long as it possesses axial symmetry. Even in the absence of strict axial symmetry, however, eq. 33 can be expected to constitute a reasonable approximation, because, for an irregular distribution, some "center of gravity" orientation about which pseudo-axial symmetry obtains should exist in most cases.

A number of illustrative axially symmetric distributions, which may constitute reasonably realistic models for restricted dynamic reorientational relaxation of fluorophores attached or adsorbed to a macromolecular substrate, are presented in Appendix C. Among them, possibilities of negative axial depolarization factors are clearly demonstrated by those models, which start in the limit of a rigid planar oscillator (corresponding, for instance, to two degenerate orthogonal transitions), which is formally allowed to perform axially symmetric vibrations out of plane.

SUMMARY

In this section the conditions under which long-range resonance energy transfer experiments lend themselves to the determination of intramolecular donor-acceptor separations are summarized and experimental protocols for evaluating this distance with known uncertainty are suggested.

As has been pointed out, the dynamic averaging regime is the preferred one and lends itself to unequivocal interpretation. In the static regime, on the other hand, since there is no luminophore depolarization, no information about the orientational distribution of the donor and acceptor can be obtained. The transfer depolarization factor alone provides no useful information about the orientation factor and thereby the D-A separation.

The intermediate averaging regime, in which the reorientational motion of the probe can in principle be separated from that of the substrate as a whole, may be interpreted in terms of the dynamic averaging case to a reasonable approximation, as discussed elsewhere (Dale and Eisinger, 1974). In the intermediate case, the transfer efficiency will always be lower than

[4]In previous publications on this topic a different nomenclature was employed: $<d>_d$ was used to represent the (dynamically averaged) axial depolarization factor $<d^x>$, while $<d'>_d$ referred to the observed factor designated here by $<d>$.

that which would obtain for the same geometry in the strict dynamic limit (compare the isotropic example in Appendix A), implying that both extrema derived for R under the dynamic limit assumption will represent overestimates. The error due solely to this effect actually increases as the distributions become more isotropic.

When extrinsic labels are used, they should be chosen to be closely approximated by the limits of either a linear or planar transition moment. The chromophores' vibrational or rotational reorientation may then be estimated by the model and the experimental methods discussed here. To measure the transfer depolarization factor, excitation into higher donor transitions should be avoided, for in such cases, as discussed at length in an earlier publication (Dale and Eisinger, 1975), the orientation and transfer depolarization factors are not correlated.

Because even a modest degree of reorientational freedom can reduce the uncertainty in $<\kappa^2>$ appreciably, it is important that the depolarization factors for both luminophores with respect to the substrate be measured as accurately as possible, preferably by determining the time dependence of the overall depolarization process directly. As discussed above, an additional measurement of $<d_T>$ serves to narrow the range of uncertainty of $<\kappa^2>$ further.

It is useful to consider three cases under which $<\kappa^2>$ from polarized intramolecular excitation energy transfer might be analyzed.

Neither $<\mathrm{d_D}>$ *Nor* $<\mathrm{d_A}>$ *Known*

$<\kappa^2>$ under these conditions may be arbitrarily close to its limits of 0 or 4. This sets a maximum separation approximately 35% higher than under the isotropic assumption ($<\kappa^2> = \frac{2}{3}$), but allows an arbitrarily small minimum separation. Knowledge of $<d_T>$ is not helpful in this case.

$<d_D>$ *and/or* $<\mathrm{d_A}>$ *Known,* $<\mathrm{d_T}>$ *Unknown*

When both donor and acceptor depolarization factors are determined, but the transfer depolarization factor is not available, the contour plot of Fig. 9 should be consulted. It is important to remember that, if one or both of the measured depolarization factors are less than 0.25, the $<d_D^x>$ and/or $<d_A^x>$ values obtained as their square roots (Eq. 33) are of unknown sign in the absence of independent information (e.g. as to whether one or the other of them corresponds to a planar transition). All combinations of possible signs must therefore be taken into consideration in determining the maximum and minimum values of $<\kappa^2>$ from this plot. The same plot may be employed when only one of the depolarization factors is known, the absolute maximum and minimum being obtained by searching along the line defined by the known $<d^x>$ through all values of the other depolarization factor.

Note that if one of the depolarization factors is determined to be zero, corresponding to complete reorientational isotropy of that luminophore, the extreme values of $<\kappa^2>$ are $\frac{4}{3}$ and $\frac{1}{3}$, so that the maximum error in R due to the assumption of $\frac{2}{3}$ for $<\kappa^2>$ is only about 12%.

$<\mathrm{d_D}>$, $<\mathrm{d_A}>$, *and* $<\mathrm{d_T}>$ *Known*

The appropriate plots from among those presented in Figs. 4–7 are chosen with due regard to any ambiguity in the sign of d_T^x, as indicated in the body of the text. The maxima and minima thus obtained represent estimates of the true and, in the absence of additional structural

information, irreducible uncertainty associated with the relative orientations of donor and acceptor moieties.

It is worth stressing again that the protocol described here is independent of the particular orientational distribution functions that may be chosen for the luminophores and requires only that they are at least approximately axially symmetric.

It should finally be mentioned that the uncertainty caused by the experimenter's ignorance of the orientation factor can, at least in principle, be overcome in certain cases. The use of a transition metal ion with a purportedly triply-degenerate transition as acceptor already reduces the uncertainty in $<\kappa^2>$ to about 12% in the worst case, i.e. when the donor transition is linear and fixed (Latt et al., 1970, 1972; Darnall et al., 1976; Birnbaum et al., 1977). The recent use of Tb^{3+}, again with a purportedly triply-degenerate transition, as the donor to Co^{2+} (Berner et al., 1975; Horrocks et al., 1975) presumably completely removed all uncertainty in $<\kappa^2>$, although the assumption of an isotropic oscillator was not reported to have been tested by a depolarization measurement or by other optical techniques. That the electronic transitions of a metal ion exhibit a single bell-shaped envelope is not sufficient ground to assume that its absorption will be isotropic. The best confirmation of isotropy is the measurement of the absorption coefficients in a single crystal of the metal-ligand complex. It is also sufficient that measurements in solution of the absorption, the circular dichroism, and the magneto-circular dichroism all can be described by a single spectral feature.

While only a few macromolecules of biological interest are likely to bind transition metal ions specifically, it should be possible to design a variety of organic chelates for these metal ions, which may then be bound to specific sites either covalently or by adsorption, as has been suggested earlier (Horrocks et al., 1975) and now accomplished (Leung and Meares, 1977). This may not always be desirable or even possible (e.g. when one or both probe moieties are intrinsic to the system). In these and all other cases, where the donor and/or acceptor lack orientational isotropy due to a degeneracy of the transition moments, the protocols described in this paper provide the narrowest possible limits to the donor-acceptor separation obtained from excitation energy transfer experiments.

APPENDIX A

Intramolecular Energy Transfer in the Limit of Static Random (Isotropic) Orientational Averaging

It can be seen from Eq. 5 that the statically averaged energy transfer efficiency between a donor and an acceptor separated by a fixed distance R is

$$<T>_s = <\kappa_{Ti}/(\tau_D^{-1} + \kappa_{Ti})> = <\kappa_i^2/(C^{-1}R^6 + \kappa_i^2)>. \quad (34)$$

As has been discussed previously (Eisinger and Dale, 1974; Dale and Eisinger, 1975, 1976), this result cannot readily be adapted, in general, to evaluate R for an ensemble of **D**, **A** pairs since the R and κ^2 dependence cannot be separated, each **D**, **A** pair having a different and unknown κ_i^2. The only exceptions occur when (*a*) $<T>_s$ is vanishingly small so that it approaches the dynamic average efficiency $<T>_d$ or (*b*) both **D** and **A** have isotropic orientational distributions. The latter situation will be considered in the following.

The static average transfer efficiency given by Eq. 34 may be rewritten as

$$<T>_s = 1 - <1/(1 + a\kappa^2)>, \quad (35)$$

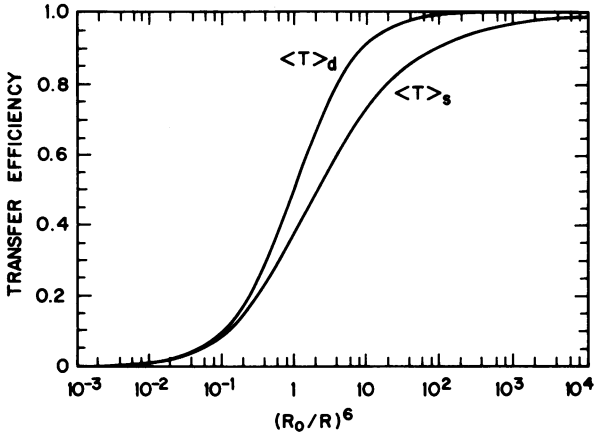

FIGURE 10 The dynamically and statically averaged transfer efficiencies, $<T>_d$ and $<T>_s$, as functions of $(R_0/R)^6$, calculated under the "isotropic assumption" for the orientational freedom of both luminophores (cf. Appendix A). The area between the curves corresponds to all averaging regimes between the static and dynamic limits. The averaging regime is seen to make little difference if the transfer efficiency is low.

where $a = CR^{-6}$. For the case under consideration, it is most convenient to express κ^2 in terms of the coupling of the donor electric field vector that makes an angle ω with the acceptor transition moment (Steinberg, 1968):

$$\kappa^2 = (3\cos^2\theta_D + 1)\cos^2\omega. \tag{36}$$

Averaging may then be accomplished by substituting $x = \cos\theta_D$ and $y = \cos\omega$ and integrating over the appropriate ranges:

$$<T>_s = 1 - \int_0^1\int_0^1 [1 + a(1 + 3x^2)\,y^2]^{-1}\,dy dx,$$

$$= 1 - \int_0^1 (1/\sqrt{b})\tan^{-1}(\sqrt{b})\,dx \tag{37}$$

where $b = a(1 + 3x^2)$. $<T>_s$ may be obtained as a function of (R_0/R), where R_0 contains an arbitrary value of κ^2 (see Eq. 2), by numerical integration of Eq. 37. The result for $\kappa^2 = \frac{2}{3}$ is displayed in Fig. 10, which also shows for comparison the corresponding dynamically averaged efficiency $<T>_d$ defined by Eq. 5 with $\kappa^2 = \frac{2}{3}$ as appropriate for the isotropic case considered.

Since in the dynamic limit all D, A orientations, including those favorable for rapid transfer, are sampled during the transfer time, $<T>_d$ always exceeds $<T>_s$ for a given intramolecular separation. The error in the intramolecular separation R, introduced by assuming the wrong averaging regime in deriving R from energy transfer efficiencies, in this case is readily seen to be about 15% when $<T>_d$ is 0.5 and about 50% when $<T>_d$ is 0.9 (cf. Fig. 10). At low transfer efficiencies the error becomes negligible, as is easily shown to be true, e.g. from Eq. 5, independently of whether the orientational distributions are isotropic or not.

APPENDIX B

Distribution of Values of the Orientation Factor

It has frequently been stated or tacitly assumed that the average value of $\frac{2}{3}$ for κ^2, which corresponds to complete dynamic isotropic orientational averaging of both **D** and **A**, is a reasonable approximation for

D-A pairs in which the **D** and **A** orientations are either fixed or incompletely averaged. It is of course doubtful whether the use of a value equal to that for a statistical average of all possible relative **D** and **A** orientations in the dynamic limit is justifiable in a particular situation. Leaving this question aside, the claims for the approximate validity of the "two-thirds" assumption can be tested by investigating the probability density and probability distribution of κ^2 under the assumption that all spatial orientations of both **D** and **A** are equally likely and that the orientation of the donor is independent of that of the acceptor.

The probability density of κ^2, $p(\kappa^2)$, will be the probability density of $(3\cos^2\theta_D + 1)\cos^2\omega$ taken over all values of θ_D and ω in Eq. 36. This is isomorphous with the probability density, $p(z)$, of $z = (3x^2 + 1)y^2$ taken over all values of x and y between 0 and 1. For any fixed value of x, $p(z)|_x$ will be proportional to $1/\sqrt{z}$ for $0 < y < (3x^2 + 1)$ as $p(z) = 1/2\sqrt{az}$ over the interval $0 < y < a$ when $z = y^2$. In the interval $1 < z < 4$, $p(z)$ may be obtained from $p(z)|_x$ by integration. Substituting $v = 3x^2 + 1$, one obtains

$$p(z)|_1 - p(z) \propto (1/\sqrt{z}) \int_z^4 [p(v)/\sqrt{v}]\,dv. \tag{38}$$

As $p(v) = \sqrt{3/(v-1)}$, the integral is $\ln(\sqrt{v-1} + \sqrt{v})$. Evaluating the constant of integration and normalizing to unit total probability gives

$$p(\kappa^2) = [2/\sqrt{3\kappa^2}]\,[\ln(2 + \sqrt{3}) - g(\kappa^2)], \tag{39}$$

where $g(\kappa^2) = 0$ for $0 < \kappa^2 < 1$ and $g(\kappa^2) = \ln(\sqrt{\kappa^2 - 1} + \sqrt{\kappa^2})$ for $1 < \kappa^2 < 4$. This probability density function is plotted in Fig. 11 and is equivalent, though simpler in form, to an expression derived elsewhere (Jones, 1970). It can be seen at a glance that the most probable value of κ^2 is zero.

The probability distribution of this density function is obtained by integrating from zero to any arbitrary value of κ^2:

$$P(\kappa^2) = \int_0^{\kappa^2} p(z)\,dz. \tag{40}$$

Substituting Eq. 39 into Eq. 40 and integrating gives

$$P(\kappa^2) = \begin{cases} \sqrt{3\kappa^2}\ln(2 + \sqrt{3}) & (0 < \kappa^2 < 1) \\ \sqrt{3\kappa^2}\,[\ln(2 + \sqrt{3}) - \sqrt{\kappa^2}\ln(\sqrt{\kappa^2} + \sqrt{\kappa^2 - 1}) - \sqrt{\kappa^2 - 1}] & (1 < \kappa^2 < 4). \end{cases} \tag{41}$$

This probability distribution function is also plotted in Fig. 11. Inspection of the latter curve shows that, for instance, there is approximately a 60% probability that κ^2 has a value outside the limits ⅓–4/3, and an almost 45% probability that it is less than ⅓. In addition, there is approximately a 20% probability that κ^2 has a value less than 0.1 of its average value of ⅔ and almost 12% probability that it is less than 0.02. The corresponding values derived for the D-A separation in the latter two cases are $0.1^{1/6}$ and $0.03^{1/6}$, i.e. about 0.68 and 0.56, of that obtained under the assumption of an average value of ⅔ for κ^2.

It has in the past been argued that the "isotropic" value of ⅔ for $<\kappa^2>$ has statistical validity for D-A pairs with unknown relative orientations, since extreme values for κ^2 (0 or 4) are unlikely to obtain for a pair of independent transition dipoles. The forgoing discussion dispels the credibility of this argument. Indeed, it shows that the opposite is true, since values of κ^2 near zero are seen to predominate in a random distribution. There exists, moreover, a fundamental objection to obtaining an estimate for the orientation factor on statistical grounds. A fluorescent label, be it intrinsic or extrinsic, is found at a specific site of a macromolecule because of the unique structural or functional properties of its interaction with the site. It is therefore likely that the resultant distribution of dipole orientations, while somewhat heterogeneous, will be characterized by a narrow range of geometries. It is quite unlikely that any particular geometry will obtain when it is calculated on the basis of probability distributions, as has been proposed recently (Hillel and Wu, 1976), even when the calculations include, as there, estimates of

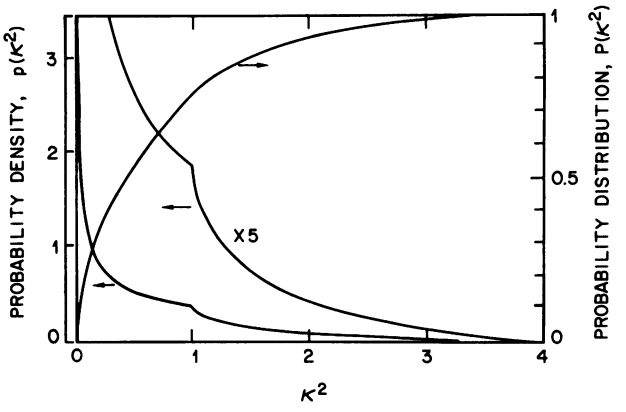

FIGURE 11 The curve $p(\kappa^2)$ gives the probability density that any particular value of κ^2 obtains between two dipoles, each of which may adopt any orientation independently of the other. $P(\kappa^2)$ is the probability distribution of κ^2 having a value between 0 and κ^2. The probability of κ^2 being less than 0.1, for example, is seen to be 0.25.

restricted dynamic orientational averaging. Only a range of possible κ^2 values can be defined as outlined in this work. Some value within this range will be the appropriate one, but it cannot be estimated more closely.

APPENDIX C

Depolarization Factors for Some Axially Symmetric Orientational Distributions

In this Appendix a number of models for a luminophore attached to a macromolecular substrate with some orientational freedom will be used to calculate the corresponding dynamically averaged axial and observed depolarization factors. Only axially symmetric distribution functions are considered, and the transition moments are assumed to be either linear, as would obtain for the lowest nondegenerate transition of a luminophore, or planar, corresponding, for instance, to two degenerate orthogonal transitions. These two limiting cases, here examined in parallel, correspond respectively to centrally and peripherally weighted angular distributions of a linear transition. In the former case the angular distribution is best defined by a radial density function $g(\psi)$, where ψ is the polar angle between the transition moment and the axis of symmetry of the distribution. It is more convenient to give the results for planar oscillators in terms of

$$\psi' = \pi/2 - \psi, \tag{42}$$

where ψ' is the angle between the planar transition dipole and the plane normal to the symmetry axis of the orientational distribution. The axial depolarization factors for a given ψ or ψ' are

$$d^x(\psi) = \tfrac{3}{2}\cos^2\psi - \tfrac{1}{2}, \tag{43}$$

or, correspondingly,

$$d^x(\psi') = \tfrac{3}{2}\sin^2\psi' - \tfrac{1}{2}. \tag{44}$$

Average axial depolarization factors for the various distributions may be obtained by integrating Eqs. 43 and 44, weighted by the appropriate radial density function and geometrical element:

$$\langle d^x \rangle = \left(\int_0^\pi d^x(\psi) g(\psi) \sin\psi \, d\psi\right) \Big/ \left(\int_0^\pi g(\psi) \sin\psi \, d\psi\right), \tag{45}$$

or, correspondingly,

$$<d^x> = \left(\int_0^{\pi/2} d^x(\psi')\, g(\psi') \cos\psi' \, d\psi'\right) \Big/ \left(\int_0^{\pi/2} g(\psi') \cos\psi' \, d\psi'\right). \tag{46}$$

The dynamically averaged observed depolarization factors $<d>$ are then, according to Eq. 33, simply the squares of these axial depolarization factors.

Free Rotation about One or More Bonds

This model is useful for examining the cumulative effects of rotation about various bonds between the luminophore and the macromolecular substrate. The radial density function for rotation about a single bond is

$$g(\psi) = \begin{cases} 1 & (\psi = \Psi) \\ 0 & (\psi \neq \Psi) \end{cases} \tag{47}$$

where Ψ is the angle between the transition dipole and the bond about which free rotation is assumed to occur. In other words, the transition moment is constrained to lie on the surface of a cone with half-angle Ψ. Then

$$<d^x> = d^x(\Psi) = \tfrac{3}{2}\cos^2\Psi - \tfrac{1}{2}, \tag{48}$$

so that

$$<d> = <d^x>^2 = (\tfrac{3}{2}\cos^2\Psi - \tfrac{1}{2})^2. \tag{49}$$

These equations have been given elsewhere (Dale and Eisinger, 1974, 1975) and are also obtainable as the limit of the expression for the time-dependence of depolarization derived much earlier for this model (Gottlieb and Wahl, 1963). Figs. 12 *a* and *b* (with $n = 1$) display these depolarization factors as functions of Ψ and illustrate the fact that they vanish, corresponding to complete depolarization, at the "magic angle"

$$\Psi_m = \cos^{-1}(1/\sqrt{3}) \simeq 54.7°. \tag{50}$$

If free rotation about several bonds is possible, Soleillet's theorem (cf. Eq. 8) permits the evaluation of the cumulative depolarization

$$<d^x_{n+1}> = d(\Psi) \prod_{i=1}^{n} d(\Psi_i) = d(\Psi)<d^x_n>, \tag{51}$$

where Ψ is, as before, the angle between the transition moment and the proximal bond about which rotation occurs, and Ψ_i are the angles between each of the n successive rotatable bonds. As always for the axially symmetric distributions considered here, the observed depolarization factor $<d_{n+1}>$ is the square of this expression. Figs. 12 *a* and *b* depict $<d^x_n>$ and $<d_n>$ for $n = 1$–6 and $\Psi_i = \Psi$ between 0 and $\pi/2$, since these functions are symmetrical about the latter angle. The time dependence of depolarization caused by multiple bond rotations has also been considered previously (Wallach, 1967).

It is of interest to generalize the forgoing model to cases in which a degree of radial vibration of amplitude ϵ about a mean angle Ψ occurs. The corresponding radial density function is then

$$g_s(\Psi) = \begin{cases} 1 & (\max(0, \Psi - \epsilon) \leq \psi \leq \min(\pi, \Psi + \epsilon)) \\ 0 & (\text{elsewhere}) \end{cases} \tag{52}$$

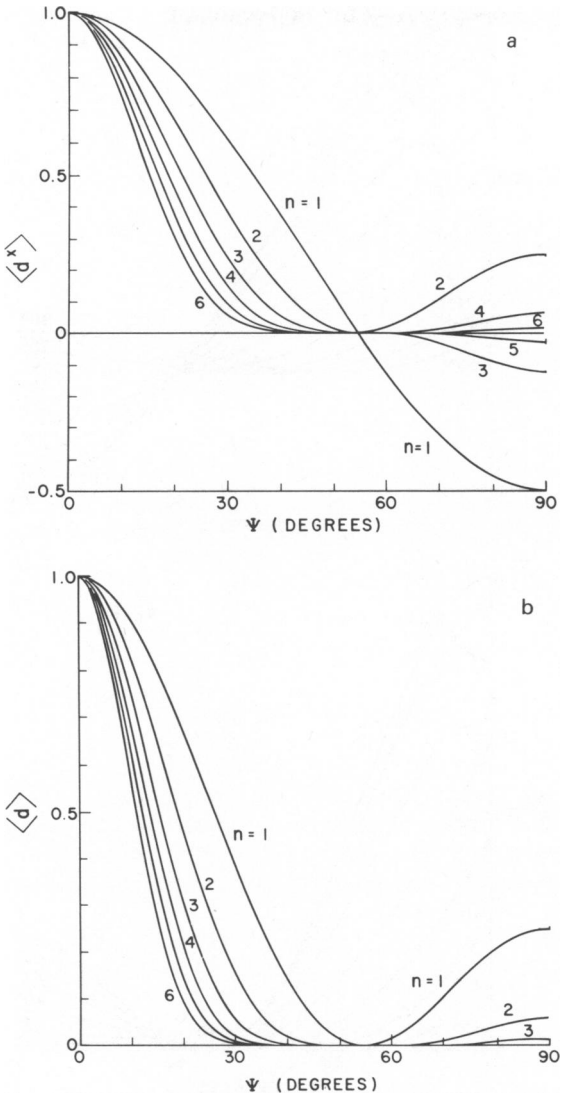

FIGURE 12 The curves labeled $n = 1$ in *a* and *b* give the axial and observed depolarization factors, respectively, for a luminophore constrained to the surface of a cone of half-angle Ψ. This orientational constraint corresponds to the existence of a single, freely rotatable bond between the luminophore and the substrate. The remaining curves, labeled $n = 2, 3, 4, 5, 6$, correspond to n equivalent rotatable bonds between luminophore and substrate and are seen to give rise to ever-decreasing depolarization factors.

with Ψ and $\epsilon \leq \pi/2$. Upon substitution into Eq. 45 and integration,

$$<d^x> = \begin{cases} \frac{3}{2}(4\cos^2\Psi\cos^2\epsilon - \cos^2\Psi - \cos^2\epsilon) & (\epsilon \leq \Psi) \\ \frac{1}{2}\cos(\Psi + \epsilon)[1 + \cos(\Psi + \epsilon)] & (\epsilon \geq \Psi). \end{cases} \quad (53)$$

These functions and the observed depolarization factors derived from them are presented in Figs. 13 *a* and *b* for a set of ϵ values. Frehland (1976) has recently considered the time-dependence of the

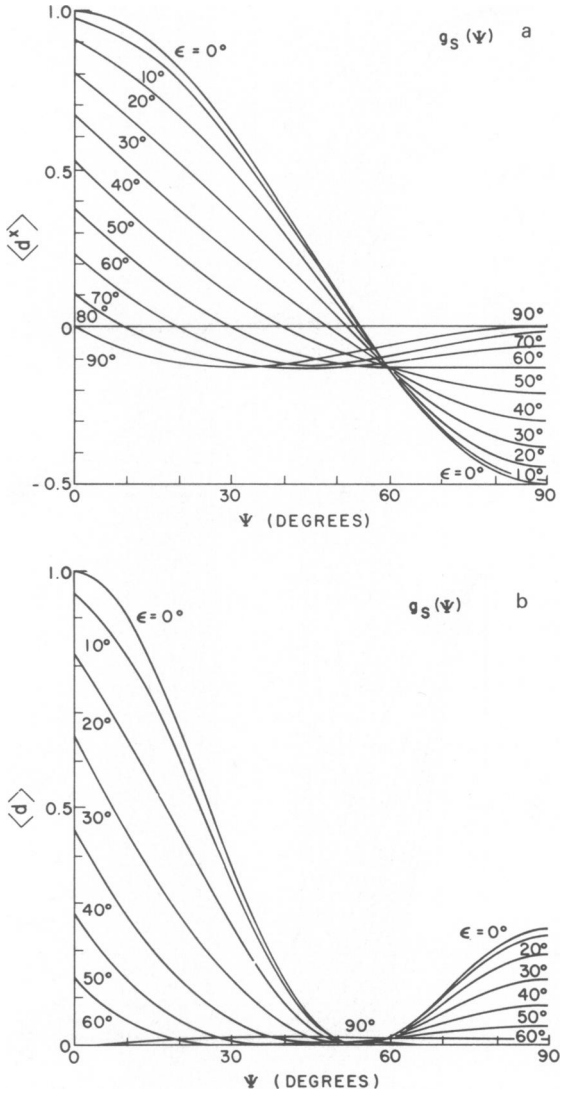

FIGURE 13 *a.* Dynamically averaged axial depolarization factors of a luminophore constrained to the volume between two cones with half angles $\Psi \pm \epsilon$. This model defined by $g_s(\psi)$ (Eq. 52) approaches the random walk model described by the distribution function $g_R(\psi)$ (see Eq. 54 and Fig. 15), when ϵ and Ψ are comparable. It corresponds to orientational isotropy with $<d> = <d^x> = 0$ when $\Psi = \epsilon = \pi/2$. *b.* Observed, dynamically averaged depolarization factors for the same model.

depolarization suffered by probes undergoing restricted rotation in anisotropic media in terms of this model.

Space-Filling Models

Only a few space-filling models with axial symmetry will be considered here. While these were chosen for illustration, some correspond to constraints imposed by simple potential wells. The radial density functions $g(\psi)$ and $g(\psi')$ for these models are displayed in Fig. 14. Analytical expressions can be derived for the depolarization factors for all except the Gaussian model. Some of these expressions are rather

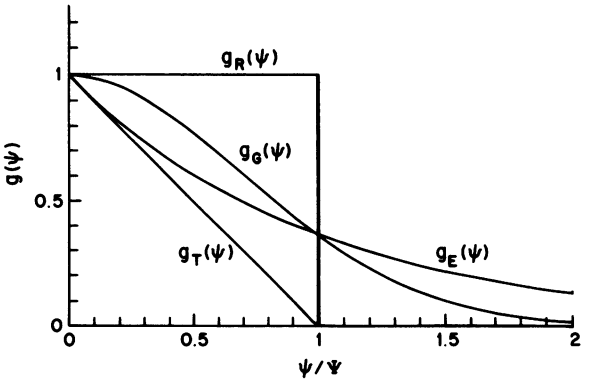

FIGURE 14 Schematic representation of the various orientational distribution functions considered in Appendix C. The curves labeled g_R, g_G, g_E, and g_T correspond to random walk, Gaussian, exponential, and triangular distributions, respectively. The angle Ψ is characteristic of the extent of each distribution and is the independent variable in Figs. 15–18, which give the depolarization factors for the various distributions.

complex and lengthy, and in practice the corresponding depolarization factors were calculated, as for the Gaussian model, by numerical integration.

MODEL I. RANDOM WALK WITHIN THE CONFINES OF A CONE OF HALF-ANGLE Ψ This model, which forms an analogue of the infinitely deep square well potential in two dimensions, is the only space-filling model considered previously in this connection (Eisinger and Dale, 1974; Dale and Eisinger, 1974, 1975; Eisinger, 1976). It corresponds to a random walk over a conical segment and has also been invoked in connection with the time dependence of restricted rotational motion of fluorescent probes in lipid bilayer membranes (Kawato et al., 1977; Kinosita et al., 1977). The radial density function is

$$g_R(\psi) = \begin{cases} 1 & (0 \leq \psi \leq \min(\Psi, \pi)) \\ 0 & (\psi > \Psi) \end{cases}, \tag{54}$$

for which the axial depolarization factor reduces to

$$<d^x> = \tfrac{1}{2} \cos \Psi (1 + \cos \Psi). \tag{55}$$

The depolarization factors computed on this basis are presented in Fig. 15 *a*.[5] The corresponding model incorporating peripheral weighting, i.e. starting in the limit of a planar transition or, equivalently, in the limit of a linear transition rotating rapidly in a plane (cf. Kinosita et al., 1977), has the radial distribution function

$$g_R(\psi') = \begin{cases} 1 & [0 \leq \psi' \leq \min(\Psi', \pi/2)] \\ 0 & (\psi > \Psi') \end{cases}, \tag{56}$$

and is characterized by the very simple axial depolarization factor

$$<d^x> = -\tfrac{1}{2} \cos^2 \Psi'. \tag{57}$$

This function is displayed, along with its square, which represents the observed depolarization factor, in Fig. 15 *b*.

[5]An error in a previous calculation of $<d>$ (designated $<d'>_d$ there) for this model in the range $(\pi/2 < \psi < \pi)$ (Dale and Eisinger, 1975) is apparent and is corrected here.

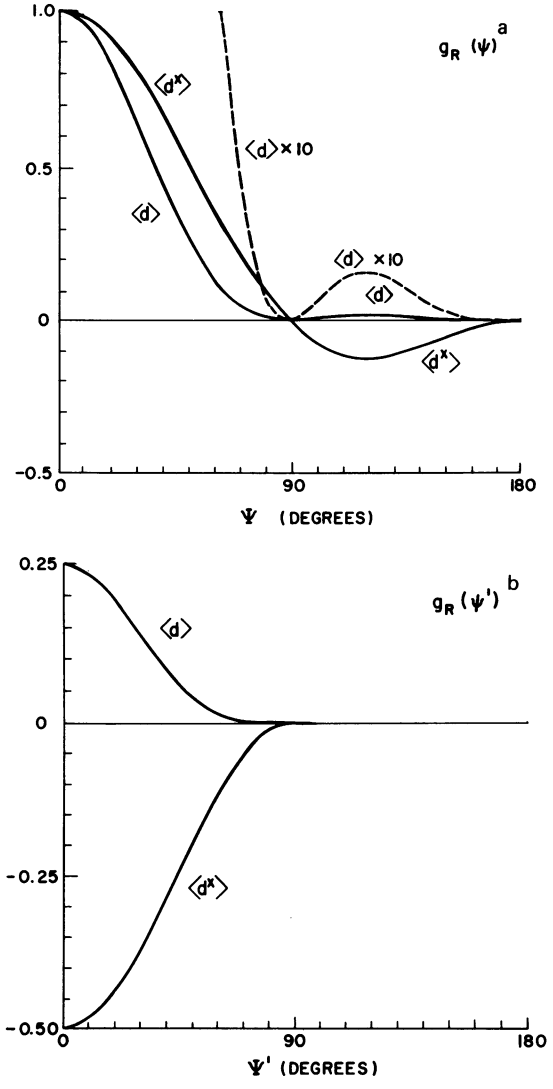

FIGURE 15 *a*. Dynamically averaged axial and observed depolarization factors, $<d^x>$ and $<d>$, for a luminophore whose linear transition moment is constrained to lie within the volume of a cone of half-angle Ψ with respect to the substrate. This is the random walk model discussed in the text. *b*. Same as *a* except that the transition moment is considered to be planar, and Ψ' is the angle between it and the plane normal to the symmetry axis of the orientational distribution, i.e. $\Psi' = (\pi/2) - \Psi$.

MODEL II. TRIANGULAR DISTRIBUTION The radial density function decreases linearly from unity at the axis or periphery ($g(\psi)$ or $g(\psi')$, respectively) to zero at the "characteristic" angle Ψ or Ψ'. Thus,

$$g_T(\psi) = \begin{cases} 1 - (\psi/\Psi) & [0 \leq \psi \leq \min(\Psi, \pi)] \\ 0 & [\psi > \min(\Psi, \pi)] \end{cases}, \tag{58}$$

and the equivalent expression in ψ', Ψ', and min $(\Psi', \pi/2)$. The resulting axial depolarization factors

$$<d^x> = \begin{cases} \frac{1}{24}\left(\frac{3 \sin \Psi - \sin (3\Psi)}{\Psi - \sin \Psi}\right) & (0 \leq \Psi \leq \pi) \\ 0 & (\Psi \geq \pi) \end{cases}, \tag{59}$$

and

$$<d^x> = \begin{cases} -\frac{1}{24}\left(\frac{4 - 3 \cos \Psi' - \cos (3\Psi')}{1 - \cos \Psi'}\right) & (0 \leq \Psi' \leq \pi/2) \\ -\frac{1}{3}\left(\frac{1}{2\Psi' - \pi + 2}\right) & (\Psi' \geq \pi/2) \end{cases}, \tag{60}$$

along with the observed depolarization factors $<d>$ derived from them are given in Figs. 16 *a* and *b*.

MODEL III. EXPONENTIAL DISTRIBUTION This model corresponds to an analogue of the two-dimensional triangular well potential. The radial density function is

$$g_E(\psi) = e^{-(\psi/\Psi)} \quad (0 \leq \psi \leq \pi), \tag{61}$$

and the equivalent for ψ' in $(0, \pi/2)$. In this case again, integration gives rise to quite simple forms for the axial depolarization factors,

$$<d^x> = 1/(1 + 9\Psi^2) \tag{62}$$

and

$$<d^x> = -\frac{1 + \Psi'(3\Psi' - 2e^{-\pi/2\Psi'})}{2(1 + 9\Psi'^2)(1 + \Psi' e^{-\pi/2\Psi'})}, \tag{63}$$

for centrally and peripherally weighted models, respectively. These and the corresponding $<d>$'s are presented in Figs. 17 *a* and *b*, in which the ranges of Ψ and Ψ' are arbitrarily restricted to π radians for comparison with the previous distribution models.

MODEL IV. GAUSSIAN DISTRIBUTION A Gaussian radial density function may constitute the most realistic of the models considered here and corresponds to an analogue of the two-dimensional parabolic well potential. The radial density function is

$$g_G(\psi) = e^{-(\psi/\Psi)^2} \quad (0 \leq \psi \leq \pi), \tag{64}$$

along with the equivalent expression for ψ' in $(0, \pi/2)$. The corresponding depolarization factors are visualized in Figs. 18 *a* and *b*. Since this distribution function is weighted more heavily centrally (ψ) or peripherally (ψ') than in the exponential model, the absolute depolarization factors as functions of the "characteristic" angles Ψ and Ψ' are much smaller than those for the exponential model shown in Figs. 17 *a* and *b*.

Of course, an infinity of distributions could be invoked in this context, although presumably only a limited number correspond to physical reality. It is important to emphasize that, for the analysis of energy transfer experiments, it is not necessary to know the precise form of the actual distributions but only to know that they have at least approximate axial symmetry.

It should finally be noted that the axial depolarization factor $<d^x>$ defined here has significance beyond its use in connection with fluorescence depolarization. Thus, it appears as the electron spin resonance order parameter for rapid anisotropic tumbling of spin labels, described in terms of some of the distribution models discussed above, e.g. the random walk model (Van et al., 1974; Israelachvili et

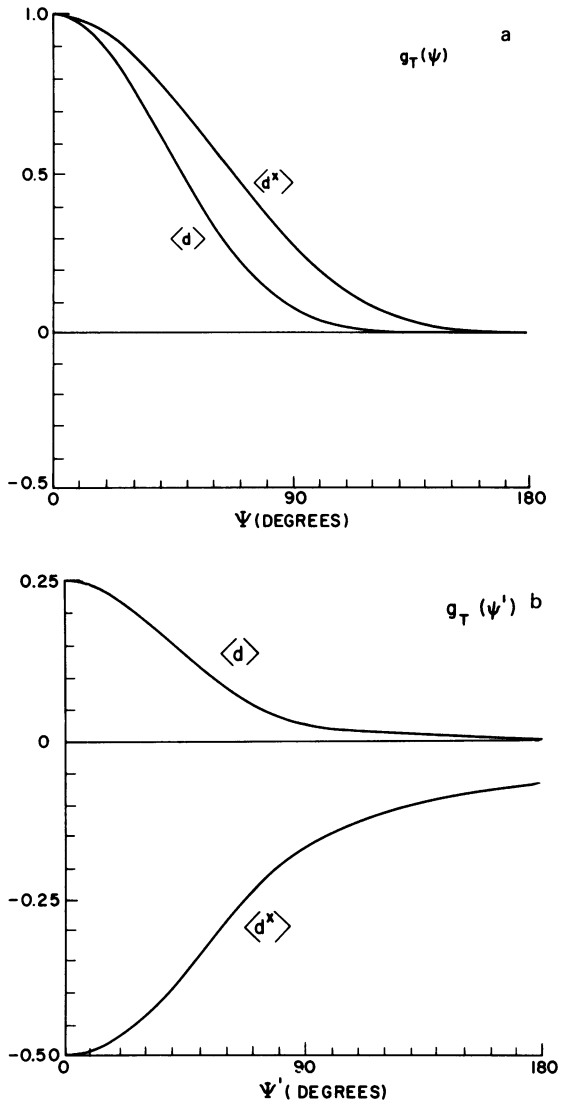

FIGURE 16 *a*. Dynamically averaged axial and observed depolarization factors, $<d^x>$ and $<d>$, for a luminophore whose linear transition moment has a triangular radial density function ($g_T(\psi)$ in Fig. 14) of characteristic angle Ψ. *b*. Same as *a* except that the transition moment is considered to be planar, and Ψ' is the angle between it and the plane normal to the symmetry axis of the orientational distribution, i.e. $\Psi' = (\pi/2) - \Psi$.

al., 1975) and the Gaussian distribution (Gaffney and McConnell, 1974). A model not considered here, that corresponding to a Gaussian spread about a mean bond rotation angle Ψ,

$$g(\psi) = e^{-[(\psi-\Psi)/\epsilon]^2} \quad (0 \leq \psi \leq \pi), \tag{65}$$

(compare Eqs. 52 and 64), has also been utilized by the last-named authors.

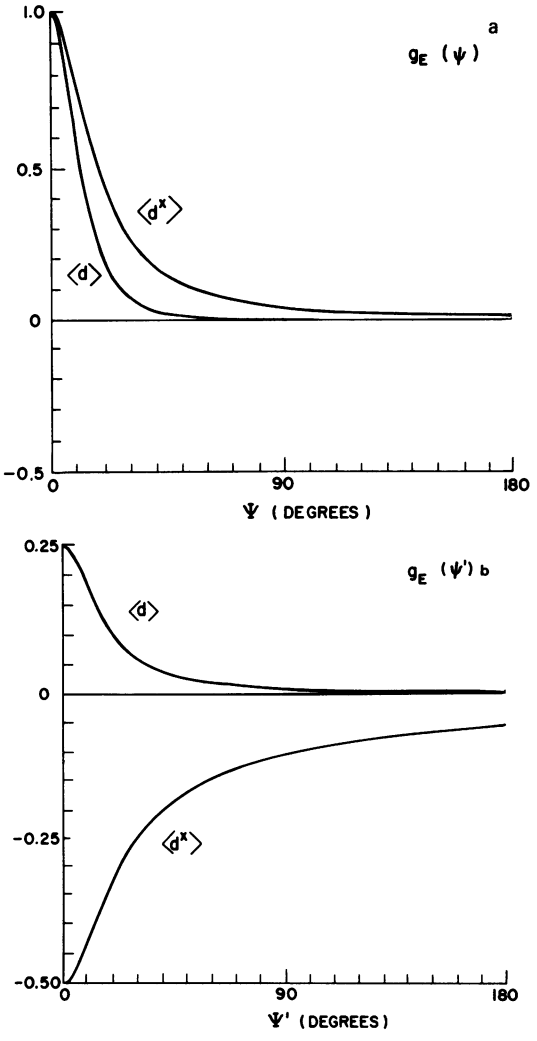

FIGURE 17 *a*. Dynamically averaged axial and observed depolarization factors, $<d^x>$ and $<d>$, for a luminophore whose linear transition moment has an exponential radial density function ($g_E(\psi)$ in Fig. 14) of characteristic angle Ψ. *b*. Same as *a* except that the transition moment is considered to be planar, and Ψ' is the angle between it and the plane normal to the symmetry axis of the orientational distribution, i.e. $\Psi' = (\pi/2) - \Psi$.

ADDENDUM

Since completion of the above in final manuscript form, a number of contributions reporting intramolecular separations using depolarization measurements to delimit upper and lower bounds have appeared in the literature (Shepherd and Hammes, 1977; Holowka and Hammes, 1977; Dockter et al., 1978; Pober et al., 1978; Tu et al., 1978; Hahn and Hammes, 1978). These have all made use of one or another of the reorientational models previously reported (Dale and Eisinger, 1974, 1975). A more complete energy transfer study of the distribution of end-to-end distances in a series of oligopeptides, including an extensive set of polarization measurements over a wide range of solvent viscosities, has also appeared (Haas et al., 1978*a*). Most recently, Haas et al. (1978*b*) have detailed a treatment of the

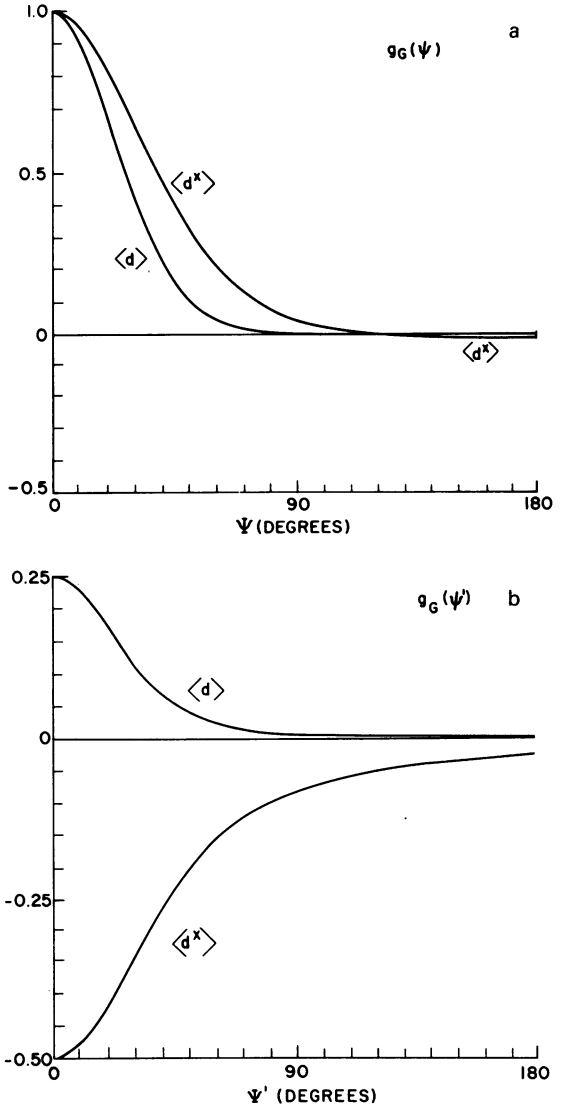

FIGURE 18 *a*. Dynamically averaged axial and observed depolarization factors, $<d^x>$ and $<d>$, for a luminophore whose linear transition moment has a Gaussian radial density function ($g_G(\psi)$ in Fig. 14) of characteristic angle Ψ. *b*. Same as *a* except that the transition moment is considered to be planar, and Ψ' is the angle between it and the plane normal to the symmetry axis of the orientational distribution, i.e. $\Psi' = (\pi/2) - \Psi$.

orientation factor problem formally equivalent to that presented here, but using directly the concept of three-dimensional transition dipole moments and formulating their results in vector form. Finally, in both that article and a recent energy transfer review (Stryer, 1978) as well as in work previously quoted (Hillel and Wu, 1976), a "statistical" argument is invoked in attempts to predict a "probable" narrower range of orientation factor values than given by the absolute upper and lower bounds obtainable directly. The applicability of this kind of approach to real situations is questionable and has been discussed here in Appendix B.

REFERENCES

ALBRECHT, A. C. 1961. Polarizations and assignments of transitions: the method of photoselection. *J. Mol. Spectrosc.* **6**:84–108.

BADLEY, R. A., W. G. MARTIN, and H. SCHNEIDER. 1973. Dynamic behavior of fluorescent probes in lipid bilayer model membranes. *Biochemistry.* **12**:268–275.

BAUGHER, J. F., L. I. GROSSWEINER, and C. LEWIS. 1974. Intramolecular energy transfer in the lysozyme-eosin complex. *J. Chem. Soc. Faraday Trans.* II. **70**:1389–1398.

BERNER, V. G., D. W. DARNALL, and E. R. BIRNBAUM. 1975. Distance measurements between the metal-binding sites in thermolysin using terbium ion as a fluorescent probe. *Biochem. Biophys. Res. Commun.* **66**:763–768.

BIRNBAUM, E. R., F. ABBOTT, J. E. GOMEZ, and D. W. DARNALL. 1977. The calcium ion binding site in bovine chymotrypsin A. *Arch. Biochem. Biophys.* **179**:469–476.

CANTOR, C. R., and P. PECHUKAS. 1971. Determination of distance distribution functions by singlet-singlet energy transfer. *Proc. Natl. Acad. Sci. U.S.A.* **68**:2099–2101.

CHANG, D. S. C., and N. FILIPESCU. 1972. Unusually weak electronic interaction between two aromatic chromophores less than 10 Å apart in a rigid model molecule. *J. Am. Chem. Soc.* **94**:4170–4175.

CONRAD, R. H., and L. BRAND. 1968. Intramolecular transfer of excitation from tryptophan to 1-dimethylamino-naphthalene-5-sulfonamide in a series of model compounds. *Biochemistry.* **7**:777–787.

DALE, R. E., and J. EISINGER. 1974. Intramolecular distances determined by energy transfer. Dependence on orientational freedom of donor and acceptor. *Biopolymers.* **13**:1573–1605.

DALE, R. E., and J. EISINGER. 1975. Polarized excitation energy transfer. *In* Biochemical Fluorescence: Concepts. R. F. Chen and H. Edelhoch, editors. Marcel Dekker, Inc., New York. **1**:115–284.

DALE, R. E., and J. EISINGER. 1976. Intramolecular energy transfer and molecular conformation. *Proc. Natl. Acad. Sci. U.S.A.* **73**:271–273.

DARNALL, D. W., F. ABBOTT, J. E. GOMEZ, and E. R. BIRNBAUM. 1976. Fluorescence energy-transfer measurements between the calcium binding site and the specific pocket of bovine trypsin using lanthanide probes. *Biochemistry.* **15**:5017–5023.

DOCKTER, M. E., A. STEINEMANN, and G. SCHATZ. 1978. Mapping of yeast cytochrome *c* oxidase by fluorescence resonance energy transfer. Distances between subunit II, heme *a*, and cytochrome *c* bound to subunit III. *J. Biol. Chem.* **253**:311–317.

EISINGER, J. 1976. Energy transfer and dynamical structure. *Q. Rev. Biophys.* **9**:21–33.

EISINGER, J., B. FEUER, and A. A. LAMOLA. 1969. Intramolecular singlet excitation transfer. Applications to polypeptides. *Biochemistry.* **8**:3908–3915.

EISINGER, J., and R. E. DALE. 1974. Interpretation of intramolecular energy transfer experiments. *J. Mol. Biol.* **84**:643–647.

FÖRSTER, Th. 1948. Zwischenmolekulare Energiewanderung und Fluoreszenz. *Ann. Physik.* **2**:55–75.

FÖRSTER, Th. 1951. Fluoreszenz organischer Verbindungen. Vandenhoek & Ruprecht. Göttingen.

FÖRSTER, Th. 1965. Delocalized excitation and excitation transfer. *In* Modern Quantum Chemistry. Part III. O. Sinanoğlu, editor. Academic Press, Inc., New York. 93–137.

FREHLAND, E. 1976. Dynamical theory of fluorescence polarization in a planar array of oriented pigment molecules. *Biophys. Chem.* **4**:65–78.

GABOR, G. 1968. Radiationless energy transfer through a polypeptide chain. *Biopolymers.* **6**:809–816.

GAFFNEY, B. J., and H. M. MCCONNELL. 1974. The paramagnetic resonance spectra of spin labels in phospholipid membranes. *J. Magn. Resonance.* **16**:1–28.

GALANIN, M. D. 1955. The problem of the effect of concentration on the luminescence of solutions. *Soviet Physics—JETP.* **1**:317–325.

GOTTLIEB, Y. Ya., and Ph. WAHL. 1963. Étude théorique de la polarisation de fluorescence des macromolécules portant un groupe émetteur mobile autour d'un axe de rotation. *J. Chim. Phys.* **60**:849–856.

GRINVALD, A., E. HAAS, and I. Z. STEINBERG. 1972. Evaluation of the distribution of distances between energy donors and acceptors by fluorescence decay. *Proc. Natl. Acad. Sci. U.S.A.* **69**:2273–2277.

HAAS, E., E. KATCHALSKI-KATZIR, and I. Z. STEINBERG. 1977. Brownian motion of the ends of flexible oligomer molecules relative to one another as estimated by energy transfer between the chains ends. *Biophys. J.* **17**:234a.

HAAS, E., E. KATCHALSKI-KATZIR, and I. Z. STEINBERG. 1978*a*. Brownian motion of the ends of oligopeptide chains in solution as estimated by energy transfer between the chain ends. *Biopolymers.* **17**:11–31.

HAAS, E., E. KATCHALSKI-KATZIR, and I. Z. STEINBERG. 1978*b*. Effect of the orientation of donor and acceptor on the probability of energy transfer involving electronic transitions of mixed polarization. *Biochemistry.* **17**:5064–5070.

HAAS, E., M. WILCHEK, E. KATCHALSKI-KATZIR, and I. Z. STEINBERG. 1975. *Proc. Natl. Acad. Sci. U.S.A.* **72**:1807–1811.

HAHN, L.-H. E., and G. G. HAMMES. 1978. Structural mapping of aspartate transcarbamoylase by fluorescence energy-transfer measurements: determination of the distance between catalytic sites of different subunits. *Biochemistry.* **17**:2423–2429.

HILLEL, Z., and C.-W. WU. 1976. Statistical interpretation of fluorescence energy transfer measurements in macromolecular systems. *Biochemistry.* **15**:2105–2113.

HOLOWKA, D. A., and G. G. HAMMES. 1977. Chemical modification and fluorescence studies of chloroplast coupling factor. *Biochemistry.* **16**:5538–5545.

HORROCKS, W. DE W. JR., B. HOLMQUIST, and B. L. VALLEE. 1975. Energy transfer between terbium (III) and cobalt (II) in thermolysin: a new class of metal-metal distance probes. *Proc. Natl. Acad. Sci. U.S.A.* **72**:4764–4768.

ISRAELACHVILI, J., J. SJÖSTEN, L. E. G. ERIKSSON, M. EHRSTRÖM, A. GRÄSLUND, and A. EHRENBERG. 1975. ESR spectral analysis of the molecular motion of spin labels in lipid bilayers and membranes based on a model in terms of two angular motional parameters and rotational correlation times. *Biochim. Biophys. Acta.* **382**:125–141.

JABŁOŃSKI, A. 1960. On the notion of emission anisotropy. *Bull. Acad. Pol. Sci., Sér. Sci. Math. Astron. Phys.* **8**:259–264.

JONES, R. E. 1970. Nanosecond fluorimetry. Ph.D. thesis. Stanford University.

KAWATO, S., K. KINOSITA, JR., and A. IKEGAMI. 1977. Dynamic structure of bilayers studied by nanosecond fluorescence techniques. *Biochemistry.* **16**:2319–2324.

KINOSITA, K., JR., S. KAWATO, and A. IKEGAMI. 1977. A theory of fluorescence polarization decay in membranes. *Biophys. J.* **20**:289–305.

LANGLOIS, R., C. C. LEE, C. R. CANTOR, R. VINCE, and S. PESTKA. 1976. The distance between two functionally significant regions of the 50S *Escherichia coli* ribosome: the erythromycin binding site and proteins L7/L12. *J. Mol. Biol.* **106**:297–313.

LATT, S. A., D. S. AULD, and B. L. VALLEE. 1970. Surveyor substrates: energy-transfer guages of active center topography during catalysis. *Proc. Natl. Acad. Sci. U.S.A.* **67**:1383–1389.

LATT, S. A., D. S. AULD, and B. L. VALLEE. 1972. Distance measurements at the active site of carboxypeptidase A during catalysis. *Biochemistry.* **11**:3015–3022.

LEUNG, C. S.-H., and C. F. MEARES. 1977. Attachment of fluorescent metal chelates to macromolecules using "bifunctional" chelating agents. *Biochem. Biophys. Res. Commun.* **75**:149–155.

LUK, C. K. 1971. Energy transfer between tryptophans and aromatic ligands in apomyoglobin. *Biopolymers.* **10**:1317–1329.

MAKSIMOV, M. Z., and I. M. ROZMAN. 1962. On energy transfer in solid solutions. *Opt. Spectrosc.* **12**:337–338.

MARÓTI, P., and L. SZALAY. 1976. Transfer of electronic excitation energy between tryptophans at the active site of lysozyme. *Acta Phys. Chem.* **21**:97–107.

OHMINE, I., R. SILBEY, and J. M. DEUTCH. 1977. Energy transfer in labeled polymer chains in semidilute solutions. *Macromolecules.* **10**:862–864.

PAPADAKIS, N., and G. G. HAMMES. 1977. Fluorescent derivatives of the pyruvate dehydrogenase component of the *Escherichia coli* pyruvate dehydrogenase complex. *Biochemistry.* **16**:1890–1896.

PERRIN, F. 1926. Polarisation de la lumière de fluorescence. Vie moyenne des molécules dans l'etat excité. *J. Phys. (Paris).* **7**:390–401.

PERRIN, F. 1936. Diminution de la polarisation de la fluorescence des solutions résultant du mouvement brownien de rotation. *Acta Physica. Pol.* **5**:335–347.

POBER, J. S., V. IWANIJ, E. REICH, and L. STRYER. 1978. Transglutaminase-catalysed insertion of a fluorescent probe into the protease-sensitive region of rhodopsin. *Biochemistry.* **17**:2163–2169.

SCHILLER, P. W. 1975. The measurement of intramolecular distances by energy transfer. *In* Biochemical Fluorescence: Concepts. R. F. Chen and H. Edelhoch, editors. Marcel Dekker, Inc. New York. **I**:285–303.

SHEPHERD, G. B., and G. G. HAMMES. 1977. Fluorescence energy transfer measurements in the pyruvate dehydrogenase multienzyme complex from *Escherichia coli* with chemically modified lipoic acid. *Biochemistry.* **16**:5234–5241.

SHEPHERD, G. B., N. PAPADAKIS, and G. G. HAMMES. 1976. Fluorescence energy-transfer measurements between coenzyme A and flavin adenine dinucleotide binding sites of the *Escherichia coli* pyruvate dehydrogenase multienzyme complex. *Biochemistry.* **15**:2888–2893.

SOLEILLET, P. 1929. Sur les paramètres caractérisant la polarisation partielle de la lumière dans les phénomènes de fluorescence. *Ann. Phys. (Paris).* **12**:23–97.

STEINBERG, I. Z. 1968. Nonradiative energy transfer in systems in which rotatory Brownian motion is frozen. *J. Chem. Phys.* **48**:2411–2413.

STRYER, L. 1978. Fluorescence energy transfer as a spectroscopic ruler. *Annu. Rev. Biochem.* **47**:819–846.

STRYER, L., and R. P. HAUGLAND. 1967. Energy transfer: a spectroscopic ruler. *Proc. Natl. Acad. Sci. U.S.A.* **58**:719–726.

TU, S.-C., C.-W. WU, and J. W. HASTINGS. 1978. Structural studies on bacterial luciferase using energy transfer and emission anisotropy. *Biochemistry.* **17**:987–993.

VAN, S. P., G. B. BIRRELL, and O. H. GRIFFITH. 1974. Rapid anisotropic motion of spin labels. Models for motion averaging of the ESR parameters. *J. Magn. Resonance.* **15**:444–459.

WALLACH, D. 1967. Effect of internal rotation on angular correlation functions. *J. Chem. Phys.* **47**:5258–5268.

WRIGHT, K., and M. TAKAHASHI. 1977. Fluorescence energy transfer between heterologous active sites of affinity-labeled aspartokinase of *Escherichia coli*. *Biochemistry.* **16**:1548–1554.

WU, C.-W., L. R. YARBROUGH, F. Y.-H. WU, and Z. HILLEL. 1976. Spatial relationships of the σ subunit and the rifampicin binding site in RNA polymerase of *Escherichia coli*. *Biochemistry.* **15**:2097–2104.

WU, C.-W., and L. STRYER. 1972. Proximity relationships in rhodopsin. *Proc. Natl. Acad. Sci. U.S.A.* **69**:1104–1108.

ZUKIN, R. S., P. R. HARTIG, and D. E. KOSHLAND, JR. 1977. Use of a distant reporter group as evidence for a conformational change in a sensory receptor. *Proc. Natl. Acad. Sci. U.S.A.* **74**:1932–1936.